

## ABSTRACT

Title of Document: FLAME SPREAD THROUGH WOODEN  
DOWLES

Zhao Zhao, Master of Science, 2014

Directed By: Assistant Professor, Michael J. Gollner,  
Department of Fire Protection Engineering

In practical applications, flammable materials are often arranged in arrays of discrete objects whose combustion properties may be different as that of a homogeneous material. In this study, the influence of spacing between arrays of wooden dowels on the rate of upward flame spread through arrays has been studied. This configuration in some ways modelled physics that similar with flame spread through wildland fuels and cable trays. A single dowel was ignited at the base of an array of birch dowels with fixed spacings of 0.75, 0.875, 1.0 and 1.5 cm and allowed to spread upwards. Flame spread along the center columns, burning duration times and horizontal flame spread were plotted and compared with previous theory (Gollner et al., 2012 and Vogel and Williams, 1970). As a result of experimental results, it was shown that flame spread rates will decrease after a critical spacing is reached, most likely due to limited availability of oxygen. Experiments on horizontally-propagating flames through dowel arrays were performed to further show this effect.

FLAME SPREAD THROUGH WOODEN DOWLES

By

Zhao Zhao

Thesis submitted to the Faculty of the Graduate School of the  
University of Maryland, College Park, in partial fulfillment  
of the requirements for the degree of  
Master of Science  
2014

Advisory Committee:  
Professor Michael J. Gollner, Chair  
Professor Stanislav Stoliarov,  
Professor James Quintiere

© Copyright by  
[Zhao Zhao]  
[2014]

## Acknowledgements

First of all, I am thankful to my advisor, Dr. Michael Gollner for his patience and guidance through every step of this project. He gives me a lot of help in conducting the experiments and analyzing the data. His extremely broad knowledge and experience was the driving force behind the development of this project. He also helped me to make good presentations.

I would like to thank Daniel Gorham whom I collaborated with on this project. In addition to performing experiments with me and helping me in the laboratory, he gives a lot of good suggestions when I had problems in the research and study. Without his collaboration, I would not be able to finish all these things successfully.

I would like to thank all my group mates. They are all interesting, knowledgeable and hardworking individuals who helped me a lot during my stay here.

I would also like to thank all the Haiqing Guo, Yi Zhang, Xi Ding and other chinese students in our department. They give me a lot support in my daily life and make the office a fun and great place to stay .My special thanks go to my parents in China for their love and support.

# Table of Contents

Acknowledgements.....	ii
Table of Contents .....	iii
List of Tables .....	iv
List of Figures .....	v
Chapter 1: Introduction .....	1
1.1 Background.....	1
1.2 Cable Tray Fires.....	2
1.3 Wildland Fire Risk.....	4
Chapter 2: Theory .....	7
2.1 Burning Theory.....	7
2.1.1 Ignition of a Solid Fuel .....	7
2.1.2 Burning of Synthetic Polymers .....	9
2.1.3 Burning of Woods.....	12
2.2 Flame Spread .....	13
2.3 Porous and Discrete Flame Spread .....	17
Chapter 3: Literature Review .....	19
3.1 Flame Propagation along Matchsticks and Paper Arrays .....	19
3.2 Flame Propagation along Cable Trays .....	26
Chapter 4: Experimental Approach .....	28
4.1 Method Summary.....	28
4.2 Experimental Setup.....	29
4.3 Test Specimens .....	33
4.4 Experimental Procedure.....	34
4.5 Analysis.....	36
Chapter 5: Experimental Results .....	37
5.1 Physical Observation .....	38
5.2 Vertical Flame Spread.....	42
5.2.1 Experimental Results .....	42
5.2.2 Analysis.....	43
5.3 Burnout Times and Burning Duration Times .....	50
5.3.1 Experimental Results .....	50
5.3.2 Analysis.....	54
5.4 Horizontal Flame Spread .....	56
5.4.1 Horizontal Experimental Results for Full Arrays .....	56
5.4.2 Horizontal spread experiments of different rows of matchsticks .....	58
5.4.3 Analysis.....	61
Chapter 6: Conclusion.....	67
Appendices.....	68
References.....	74

## List of Tables

Table 1.1 Sever fire incidents involving cables

Table 1.2 Recent wildland fires in the United States

Table 2.1 Decomposition temperatures of different components in wood

Table 4.1 Experimental configurations

Table 4.2 Experimental setup and initial conditions

Table 5.1 Values of properties used in burning duration time calculations

Table 5.2 Values of properties used in ignition time calculations

## List of Figures

Figure 2.1 Factors involved in ignition of a solid material.

Figure 2.2 Physical and chemical processes in the flaming combustion of a polymer

Figure 3.1 Flame propagation along a linear matchstick array from Vogel and Williams

Figure 3.2 Features of the fire spread experimental apparatus used by Emmons and Shen between horizontal strips of paper

Figure 3.3 Details of the wind tunnel and firebed used by Prah1 and Tien

Figure 3.4 Details of firebed used by Prah1 and Tien

Figure 3.5 Side (top) and front (bottom) video showing the fire behavior observed during Gonller et al. 'experiments

Figure 3.6: Upward fire spread in a stack of horizontal open-bottom trays filled with cables

Figure 4.1: Experimental setup and aluminum plates used to hold array of wooden dowels

Figure 4.2 Pre-drilled aluminum plate with spacing of 0.875 cm

Figure 4.3 Experimental apparatus used with a 1.0 cm spacing plate

Figure 5.1 Front video showing a time-lapse of the behavior of experiments with a spacing of 1.5 cm. Note only the center row of matchsticks ignite during the spread process

Figure 5.2 Side video showing a time-lapse of the behavior of experiments with a spacing of 1.0 cm. Note that a majority of flame spread occur in the vertical direction,

however some wooden dowels to the left and right of the center column begin to ignite.

Figure 5.3 Side video showing a time-lapse of the behavior of experiments with a spacing of 0.875 cm. Note that from the base of the experiments, flame spread immediately starts to spread horizontally, eventually involving the whole array.

Figure 5.4 Front video showing a time-lapse of the behavior of experiments with a spacing of 0.75 cm. Note that flame spread, from the base, occur both vertically and horizontally, eventually involving entire array.

Figure 5.5 Progression of the pyrolysis front. Symbols indicates the location of the pyrolysis front observed from the high speed video and dashed lines indicate power-law fit to these data.

Figure 5.6 Calculated ignition times using convection heat transfer correlations (symbol with dash line) are compared with power-law fits to experimental data (symbol with solid line)

Figure 5.7 Burnout times through the center column of the array

Figure 5.8 Burning duration times. Experimental data are shown by symbols and predictions are shown as a dashed line.

Figure 5.9 Horizontal flames spread in full arrays

Figure 5.10 No horizontal flame spread behaviors happened with a spacing of 0.875 cm in 2 rows

Figure 5.11 No horizontal flame spread behaviors happened with a spacing of 0.875 cm in 3 rows.

Figure 5.12 Horizontal flame spread behaviors with a spacing of 0.875 cm in 4 rows

Figure 5.13 Horizontal spread behavior with a spacing of 0.875 cm in 5 rows.

Figure 5.14 Horizontal flame spread behavior with a spacing of 0.875 cm in 7 rows.

Figure 5.15 Horizontal flame spread with a spacing of 0.75 cm in different rows.

Figure 5.16 Horizontal flame spread with a spacing of 0.875 cm in different rows.

# Chapter 1: Introduction

## 1.1 Background

While fire is a very common phenomenon almost everyone utilizes for heating or power, it also has the capability of growing out of control, presenting a dangerous situation to human lives and properties. While fire was studied scientifically as early as Faraday, further understanding of fire aids and promotes human welfare, whether utilizing fuel more efficiently or preventing fire-related disasters. To create a general understanding, scientists often give a qualitative description of fire as a distribution of flammable material which mixes with air, is heated, and reacts, exothermically. However, to get a more quantitative description of fire, work still needs to be done. Experimental data should be obtained under a wide range of conditions and correlated with appropriate parameters. The fire process can be divided into elements which each can be calculated using basic laws of nature [1].

This study here will focus on fire spread, where buoyant flows aids the heat transfer to a burning fuel, advancing the fire front at a rate that typically accelerates with time. The study extends the previous work by Gollner et al. [2], trying to compare new results to an existing theory and quantifying the influence of whole arrays of discrete objects on flame spread. In this study, a laboratory experiment is used as a scale model of a full-scale scenario, trying to find the fundamental mechanisms of fire spread phenomenon through different materials in complex configurations.

## 1.2 Cable Tray Fires

Electric cables are ubiquitous in both high technology and household applications. It also plays critical functions in nuclear power plants (NPP) and telephone-switching buildings. Power cables provide electricity to machines such as motors, transformers and heaters. Control and instrumentation cables also connect plant equipment as switches, relays and contacts [3].

Electrical cable insulating materials present a serious hazard as a fire fuel load located adjacent to a potential ignition source (the cable itself). Insulation on these cables consist of a variety of thermoplastic and thermoset polymer, which can be an intervening combustible during a fire. Electric cables have been a key factor in many fires in NPPs over the years. For example, in 1975, a major electrical cable system fire occurred at the Brown Ferry Nuclear Plant run by the Tennessee Valley Authority. The fire was started by an employee who was using a candle to check for air leaks through a fire wall penetration seal [4]. The fire was not been put out until seven hours after ignition and caused damage to over 1600 cables, resulting in the shutdown of two nuclear generating units for more than a year. The damage was extensive because of the flammability of the cables, characterized by ease of ignition and flame spread properties. Property damage to the facility was estimated at about 10 million dollars (US), and the cost of replacement power was approximately 10 million dollars (US) each month [4]. Table 1.1 also shows some other fires involving cable trays.

Table 1.1: Sever Fire Incidents involving cables [4]

<b>Affected Plant Unit</b>	<b>Incident Date</b>	<b>Fire Type</b>
San Onofre, Unit1 (USA)	12/03/1968	Self-ignited cable fire resulting from changes in cable layout (size).
Greifswald, Unit 1	07/12/1975	Large switchgear and cable fire.
Beloyarsk, Unit 2 (Russia)	31/12/1978	Large cable fire in turbine hall propagating to other plant areas resulting in severe damage of redundant instrumentation.
South Ukraine, Unit 2 (Ukraine)	14/12/1984	Cable fire inside containment propagating to various plant areas.
Kalinin, Unit 1 (Russia)	18/12/1984	Large turbine hall fire with several pilot fires at a power cable.
Ignalina, Unit 2 (Lithuania)	05/09/1988	Large cable fire by self-ignition causing damage of various cables.
Waterford, Unit 3 (USA)	10/06/1995	Switchgear fire propagating via vertical cables and a fire barrier to horizontal cable trays.

While there has been significant improvement in the safety of cable due to added fire retardants in cables and enhanced testing and regulations, the growing use of large trays of electrical cable (e.g. server rooms) and their critical roles in safety create a pressing need for further study. Ongoing work on electrical cable tray fires has sought to accordingly predict damage patterns, rates of spread and total heat-release rates that may be aided by a small-scale modeling tool such as the one proposed here.

### 1.3 Wildland Fire Risk

A wildland fire is a fire in an area of flammable vegetation that happens in a wilderness area whether it is an uncontrolled fire occurring normally or an intentionally prescribed fire for fuel maintenance. Wildland fires have been a primary disturbance affecting occupants, fire fighters and communities surrounding wildlands (dubbed the wildland-urban interface or WUI). A wildland fire is different from other kinds of fires because of its extensive size, the speed at which it spreads out from its original source, its probability to change spread direction unexpectedly, and its ability to jump gaps such as roads and rivers. A significant increase in wildland fires are predicted in the United States, South Africa and other parts around the world. In the United States, typically there are between 60,000 and 80,000 wildfires that occur every year, burning 3 to 10 million acres of land per year [5]. While it is almost impossible to eliminate the occurrence of wildfires worldwide, there are several efforts order ways to predict and reduce the risk and occurrence of wildfires near critical WUI communities. When it comes to risk, it can be defined as the probability for the occurrence of uncontrolled, adverse consequences to human life, health, property or the environment. In other words, risk is the exposure to a chance of loss of something we value. So the wildland fire risk refers to two aspect: (1) the chance a wildland fire will occur in that area and (2) the potential loss of human values if it does. Table 1.2 shows some wildland fires which happened in recent years causing a considerable amount of loss.

The hazard of a wildland fire involves many features. First, the burning of the fire damage many natural resources if the fuel loads in the environment are not

maintained. The environmental damage occurring from large wildland fires can be disastrous, including smoke generated by the fires limiting the visibility, with toxic gases posing risks to local communities. Lives have been lost in such situations where occupants don't evacuate in time and responding firefighters are trying to limit the spread of the fires (e.g. Yanell Hill Fire [6]).

Table 1.2: Recent Wildland Fires in the United States

<b>Year</b>	<b>Size (acres)</b>	<b>Name</b>	<b>Area</b>	<b>Effects</b>
2013	25,332	Rim Fire	California	Occurred in Yosemite National Park. Biggest wildfire on record in the Sierra Nevada, and third largest wildfire in California history. The city of San Francisco went into a state of emergency.
2013	14,280	Black Forest Fire	Colorado	Large, fast-spreading fire due to dry conditions, high heat and restless winds. The fire has destroyed 509 homes and left 17 homes partially damaged. As of June 13, 2013 it became the most destructive fire in Colorado state history. The estimates of damage are expected to exceed \$90 million.
2012	18,247	Waldo Canyon Fire	Colorado	Located near Pikes Peak, north and west of Colorado Springs in the Waldo Canyon. Destroyed 346 homes making it the second most destructive fire in state history. Two fatalities reported.
2012	297,845	Whitewater-Baldy Complex Fire	New Mexico	Largest wildfire in New Mexico state history. Began in the Gila Wilderness as two separate fires that converged, both caused by lightning. Destroyed 12 homes

				in Willow Creek, NM.
2011	34,000	Bastrop County Complex Fire	Texas	The fire caused two confirmed deaths in the Bastrop area, and destroyed 1,691 residential structures, more than any other single fire in Texas history. The cost of the removal of fire debris was estimated at \$25 million.

Modeling has become a useful tool in wildland fire research, especially for predicting the spread and quantifying risk. Wildland fires are driven by complicated physics and chemical processes, occurring at different scales ranging from micrometers to kilometers. Because of the uncertainty, imprecision and scarcity of input measurements, many operational wildland fire models can't be used as a perfect form for the spread of wild fire. Currently, the fundamental mechanisms responsible for wild fire ignition and fire spread have not been explained very explicitly. In developing a better model for flame spread, fundamentally understanding fire propagation between discrete elements will be provided here.

## Chapter 2: Theory

### 2.1 Burning Theory

Fire is a rapid oxidation of a material in the exothermic chemical process of combustion, releasing heat, light, and various reaction products. It is an interaction of heat, fuel and oxygen. Small fires become larger fires by flame propagation. How a material ignites and burns is a complex process which has been studied for years. When a solid material's surface is exposed to a heat source and receives enough energy, flammable vapors are produced through chemical decomposition (pyrolysis). A small thermal source can then lead to ignition of the vapor and oxygen mixture when the concentration of flammable vapors becomes high enough. If the heat generated by the flame or another existing energy source is able to maintain the necessary flow of flammable vapors from the solid material to the gas phase, sustained combustion of the fuel will occur [7].

#### 2.1.1 Ignition of a Solid Fuel

To get a better understanding of the factors controlling the ignition of a solid material, several steps are outlined below to explain the process. Important factors in ignition are shown illustratively in Figure 2.1 [7].

First, a solid material is exposed to a heat source, raising its temperature enough to chemically decompose pyrolysis products including gaseous fuels. This decomposition procedure can be described as an idealized Arrhenius-type reaction,

$$\dot{m}_F'' = A_s e^{-E_s/(RT)}, \quad (2.1)$$

where  $A_s$  is the pre-factor,  $E_s$  is the activation energy and  $R$  is the universal gas constant.  $A_s$  and  $E_s$  are properties of the solid material. The Arrhenius equation is a nonlinear function of temperature where a critical pyrolysis temperature,  $T_{py}$  may exist to allow a critical rate of production of pyrolysis vapor.

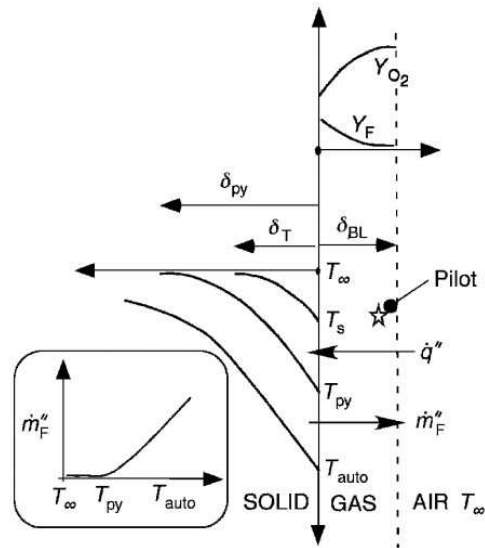


Figure 2.1 Factors involved in ignition of a solid material [7].

sufficient for ignition to occur. For a heated flat solid material, Equation 2.1 can be adapted as

$$\dot{m}_F'' = \int_0^{\delta_{py}} A_s e^{-E_s/(RT)} dx, \quad (2.2)$$

where  $\delta_{py}$  is the critical heated depth. As shown in Figure 2.1, before the temperature reaches  $T_{py}$ ,  $\dot{m}_F''$  does not increase much, however when the temperature reaches  $T_{py}$ ,  $\dot{m}_F''$  has a drastic enough increase to allow for a piloted ignition. Alternate definitions of ignition to the pyrolysis temperature also exist, such as the critical mass-loss rate for ignition [9] and are related in a similar manner.

If piloted ignition is considered, then at  $T_{py}$ , a sufficient  $\dot{m}_F''$  is released out of the surface of the material. The gaseous fuel will typically diffuse via turbulent natural convection unless the fire size is so small that mass diffusion dominates, mixing with ambient air in a thin laminar flame shear within the boundary layer. This process will take some time to reach the ignition energy, so the surface temperature will continue to rise.

Last, when the combustible mixture is in contact with a heat source, there will be an additional delay for the chemical reaction to reach a flaming condition.

This three-step process leads us to an expression for the time to ignition as

$$t_{ig} = t_{py} + t_{mix} + t_{chem}, \quad (2.3)$$

where  $t_{py}$  is the conduction heating time for the solid to reach  $T_{py}$ ,  $t_{mix}$  is the time needed for the flammable gas to reach the piloted ignition source and  $t_{chem}$  is the time for the flammable mixture to proceed to combustion at the piloted ignition source.

### 2.1.2 Burning of Synthetic Polymers

Polymers are a large and growing fraction of the fire load in household applications, commercial environments and transportation. The combination of

customizable mechanical properties, low weight, and easy processability makes them an important part of today's modern society. Most commonly used polymers contain a large fraction of carbon and hydrogen atoms, which makes their composition similar to that of a fossil fuel [9].

As mentioned above, polymers are composed of large molecules with the same intermolecular and intramolecular forces as low molecular weight compounds. These chemical bonds need more energy to be broken to produce volatile fuel matters. A significant and continuous supply of thermal energy is also needed for ignition and sustained burning in this process [10].

Generally, flaming combustion of polymers involves both physical and chemical processes taking place in three phases, the gas, interphase, and condensed phase. The interphase is described as the intermedia between the gas and condensed phase during burning. An example of a horizontal polymer slab burning with a diffusion flame is shown in Figure 2.2. On the left-hand side, the physical processes are shown which contains (1) energy transfer between the gas phase and the interphase and (2) energy loss from the interphase into the condensed phase. When burning at typical burning rates, the polymer surface retreats at a velocity of about 10<sup>-6</sup> m/s. Fuel gases are generated at a relatively low velocity ( $\approx 10^{-3}$  m/s) compared to the burning velocity of these flammable gases when mixed with air ( $\approx 1$  m/s). Accordingly, the fuel production is the rate limiting step in polymer flaming combustion, and it is governed primarily by the rate at which heat and mass are transferred to and from the polymer, respectively.

The chemical processes are shown in the right-hand side of Figure 2.2, which contain (1) thermal degradation of the polymer in the interphase as the result of energy transfer, (2) mixing of the gaseous fuel with air by diffusion, and (3) burning of the flammable gas mixture in a combustion zone. The combustion zone begins within a fuel-rich region toward the middle of the polymer and ends at a fuel-lean region on the outside. The chemical and physical processes of flaming combustion particular to each of the gas, intermedia, and condensed phases are treated separately.

Significant parameters that determine the burning rate have already been developed in the following equation [11]:

$$\dot{m}'' = \frac{\dot{Q}_F'' - \dot{Q}_L''}{L_V}, \quad (2.4)$$

where  $\dot{Q}_F''$  and  $\dot{Q}_L''$  refer to the heat flux from the flame and heat flux loss from the surface, and  $L_V$  is the heat of gasification. Equation 2.4 is assumed to apply to a quasi-steady state. The heat loss term  $\dot{Q}_L''$  is transient as it contains conductive losses via the solid which will diminish with time as the solid heats. Because of the high temperature of the polymer's surface, radiative heat loss from the material is very large. If  $L_V$  is presented for a noncharring material, it can be valid under steady burning and the noncharring material might be considered as having all fuel converted to vapor products. Otherwise, between the polymer material and the fuel phase, there is a layer of char which will thermally shield the unaffected fuel beneath. The charring layer will cause even higher temperatures and the burning behavior may consequently change, leaving only a fraction of the material that can be converted into a flammable gas.

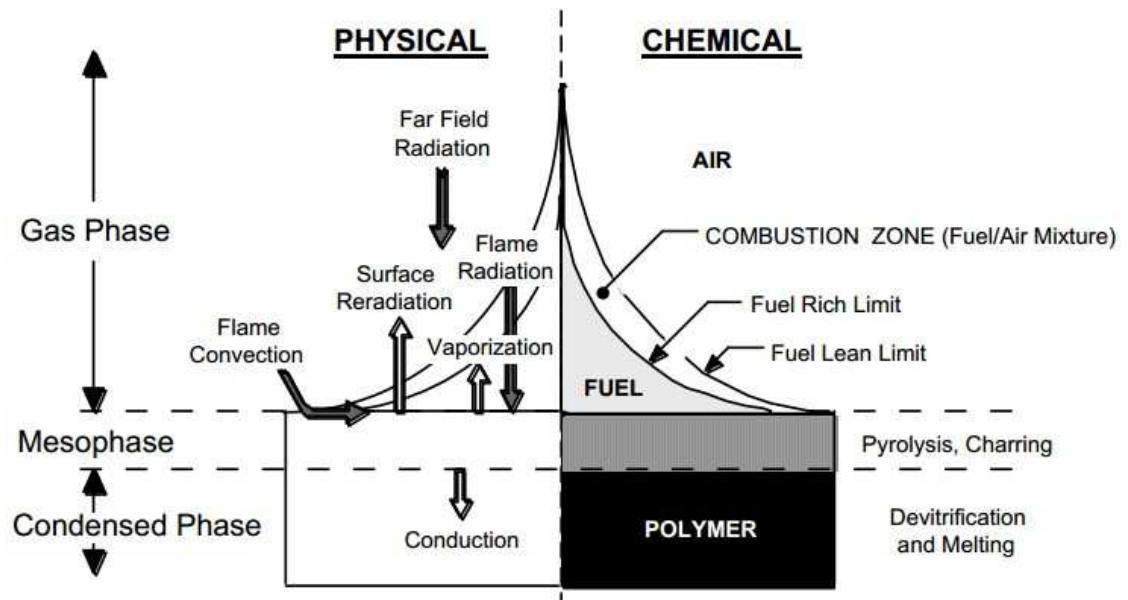


Figure 2.2 Physical and chemical processes in the flaming combustion of a polymer

[10].

### 2.1.3 Burning of Woods

Unlike synthetic polymers, wood is a natural polymer which is inhomogeneous and nonisotropic, mostly composed of cellulose, hemicellulose and lignin. These three components will decompose at different temperatures as shown in Table 2.1, releasing volatile compounds [12]. Therefore, wood products don't naturally have a fixed ignition temperature, the burning instead occurring over a range, where the probability of ignition eventually becomes high enough to occur.

Table 2.1: Decomposition temperatures of different components in wood [13]

<b>Substance</b>	<b>Decomposition Temperature</b>
Hemicellulose	200-260 °C
Cellulose	240-350 °C
Lignin	280-500 °C

When wood is exposed to a heat source, water first starts to evaporate from the surface of the wood. With gasification beginning at the wood surface and the temperature deeper inside the wood continuing to rise, evaporation of water will occur from the interior of the wood. As this behavior continues, the area that is pyrolysed spreads into the wood [13]. Lignocellulosic materials decompose in 2 sequential processes. First, under 300°C, degradation of the polymers occurs by the breaking of internal chemical bonds, dehydration, formations of free radicals, formation of carbon monoxide and carbon dioxide, and formation of reactive carbonaceous char. Second, over about 300°C, the breaking of secondary chemical bonds occurs, including the formation of intermediate products, such as anhydromonosaccharides, oligosaccharides and polysaccharides. The combustion process then proceeds similar to what happens in a polymer material as described above.

## 2.2 Flame Spread

The fire hazard of a flammable material relies on many factors such as its ignitibility, heat-release rates and flame spread rate. Because the growth of a fire, including its heat-release rate depends on flame spread, it is critical to understand the rate at which a fire spreads under many different scenarios. Flame spread can be described as a forward-propagating front where the leading edge of the flame plays a

role as both the heat source raising the fuel ahead of the flame front to its ignition temperature and also as the source of piloted ignition. There are many parameters which are known to be important in determining the rate of flame spread over flammable solids, including both material and environmental factors [14].

Material factors include both chemical and physical features of the flammable material. The chemical factors refer to the composition of the fuel and the presence of flame retardants causing effects such as solid phase charring which may insulate the material or gas-phase flame retardants which chemically inhibit the flame. The physical factors include the fuel's initial temperature, thickness, thermal properties, geometry and environmental factors consisting of the composition of the atmosphere, its temperature, existing heat sources and the surrounding air velocity. The composition of the atmosphere generally refers to the oxygen concentration in the air. If the oxygen concentration is high, materials tend to ignite more easily, resulting in flames spreading faster and materials burning at a higher rate due to an increased reaction rate and flame temperature. With an increasing temperature of the fuel, the flame spread rate also increases, as the higher the initial fuel temperature requires less energy to raise the unburnt fuel to a sustainable ignition temperature ahead of the flame. An existing heat source will also preheat the fuel surface which will lead to an increase in the rate of flame spread.

Fire researchers often simplify the complexity of the complex chemical process occurring in both the gas and solid phases while studying flame spread, instead relying on the results of simplified methods and empirical correlations from small-scale fire tests which are useful in the evaluation of the fire hazard of a given

material. To simplify interpretation of these key processes, the flame spread process is considered here as a one-dimensional flame propagation. An energy conservation equation encompassing a flame front can be written as [15]

$$\rho V \Delta h = \dot{q}'' , \quad (2.5)$$

where  $V$  is the flame spread rate,  $\rho$  is the density of the fuel,  $\dot{q}''$  is the rate of heat-transfer per unit area to unignited fuel and  $\Delta h$  is the difference in thermal enthalpy (per unit mass) between the fuel at its ignition temperature and its initial temperature, which can be expressed as [15]

$$\Delta h = c_{\rho}(T_i - T_0), \quad (2.6)$$

where  $T_i$  is the ignition temperature of the fuel,  $T_0$  is the initial temperature of the flammable material and  $c_{\rho}$  is the average heat capacity (per unit mass) between  $T_i$  and  $T_0$ . Here the ignition temperature is defined as the maximum fuel temperature on the surface of fire inception. Applying Equation 2.6 to Equation 2.5 then results in the flame spread rate,  $V$  expressed as

$$V = \frac{\dot{q}''}{c_{\rho}(T_i - T_0)\rho}, \quad (2.7)$$

Based on Equation 2.7, the flame spread rate depends on  $\dot{q}''$ , the heat energy transfer rate to a given surface per unit area, the material properties and the initial temperature. As we can generally define the material properties and initial temperature, the rate of heat transfer  $\dot{q}''$ , will become the controlling mechanism of flame spread in Equation 2.7 and also the primary concerns of this study.

Flame spread over a solid material can be divided into two regimes: thermally thin and thermally thick. For a thermally thin solid, it is assumed that there are no spatial temperature gradients inside the material. The prerequisite is that the thickness of the solid,  $d$  is less than the thermal penetration depth  $\delta_T$ ,

$$d \ll \delta_T \approx \sqrt{\alpha t} \approx \frac{k(T_s - T_0)}{\dot{q}''}, \quad (2.8)$$

where  $\alpha$  is the thermal diffusivity and  $t$  is the time the area of the material sustain a heat.

Then, for small ignition times, the time to ignition is

$$t_{ig} \approx \frac{\rho c_p d (T_{ig} - T_0)}{\dot{q}_e''}, \quad (2.9)$$

where  $\dot{q}_e''$  is the external incident heat flux.

For a thermally thick material, the thickness of the material must be

$$d \gg \delta_T \approx \sqrt{\alpha t}, \quad (2.10)$$

which for small ignition times is

$$t_{ig} \approx \frac{\pi}{4} k \rho c \left( \frac{T_{ig} - T_0}{\dot{q}_e''} \right)^2, \quad (2.11)$$

where  $k\rho c$  is the thermal conductivity, density and specific heat capacity of the solid fuel respectively.

### 2.3 Porous and Discrete Flame Spread

In wildland fires, flame propagation occurs along a discontinuous fuel bed, often defined as a porous fuel where fuel particles are relatively homogeneous. Pagni and Thomas [16], for example presented a method to predict a steady-state flame spread rate through a thin, porous layer of fuel, assumed to be a one-dimensional, homogeneous, porous fuel layer. The rate of energy transfer from the combustion zone to the fuel is assumed to dominate the rate of flame spread. The energy-transfer mechanisms assumed to preheat the fuel included flame and ember radiation, surface and internal convection, turbulent diffusion of flame eddies and gas-phase conduction [16]. Ambient flow, fuel moisture, fuel bed slope and endothermic pyrolysis were also considered in the analysis. The results of their tests lead to conclusions that without ambient flow, the controlling preheating mechanism is flame radiation, with a contribution of ember radiation and gas-phase conduction, however with the presence of ambient flow, the dominant preheating mechanism becomes a combination of convection along with a considerable contribution from flame radiation, where energy transfer by turbulent flame eddies and the energy absorbed by pyrolysis prior to ignition can be neglected.

More recently Finney et al. conducted a set of laboratory experiments in discontinuous fuel beds where the gap structure, depth and slope were varied [19]. Fires in these fuel beds showed that thresholds exist for horizontal spread which depend on environmental factors such as the ambient wind, fuel moisture content and depth of the fuel bed made of fine fuel (excelsior). For experiments with and without wind in discrete fuel beds, fire propagation occurred only after direct flame contact.

It can be summarized from the previous studies that the difference between discrete and porous fuel materials lies in which factor is treated as the primary controlling factor in pre-heating the fuel and thus flame propagation. In the burning of fine discrete materials, the net radiative heating appears insufficient for fire spread so that convective heat transfer plays an important role in fire spread. In denser material, which might be defined as porous, without forced convection, the controlling mechanism is flame radiation. These analyses have broad implications for method used to model fire propagation, particularly the importance of convective heat transfer and the features of flames distinguishing both discrete and porous fuel types [18].

In the real world, many materials are often placed in arrays of discrete patterns whose combustion properties may be different than that of a homogeneous material. Because of safety hazards, economical factors, and the difficulties of controlling boundary conditions, a full-scale experiment is not always applicable. A laboratory scale model may instead be used as a scale model of a full-scale experiment. To find the fundamental mechanisms responsible for fire propagation, matchsticks, paper arrays and other fine fuel arrays have been employed in laboratory experiments to determine the properties of fire spread behavior [19].

## Chapter 3: Literature Review

Many studies have been devoted to modelling flame spread along both thermally thin and thick solid materials. Spread experiments through discrete fuel elements have been conducted in vertical, horizontal and sloped configurations. A theory was developed using a constant ignition temperature and a flame standoff-distance profile, which achieved remarkable agreement with experimental results, suggesting that convective effects dominate in experiments at laboratory scale [20]. Some later studies were also conducted in modified and larger configurations. Also, some buoyancy effects have been incorporated into the experimental and theoretical aspects of fire spread through discrete fuel elements.

### *3.1 Flame Propagation along Matchsticks and Paper Arrays*

Arrays of wooden dowels have proved to be a useful method to model small-scale fire spread phenomena between discrete fuel elements. Although real fires may be larger and more turbulent than those conducted at laboratory scale with these small fuels, much can still be learned from lab these experiments, especially about the fundamental mechanisms of fire spread between discrete fuels. Then similarity to some wildland fuels also leads to a great analogy with which to study wildland fire spread behavior [21].

Before using matchstick arrays, Fons presented a method to investigate how a wood cylinder ignites under rapid heating [22], similar to fire conditions present in wildland and structure fires. The time required for self-ignition of a wooden cylinder was recorded and the internal temperatures observed during the ignition period of a wood cylinder inserted in a furnace were presented. The ignition time was defined as the time interval between insertion of the specimen and the first appearance of a flame. Different furnace temperatures and sizes of the specimen were used to record effects on the time of ignition. With an increase of the diameter of the specimen, the ignition time decreased as  $t_i \sim 1/\sqrt{d}$ . Also, the results showed that the rate of heating affects the ignition time significantly. Given the relationships, the ignition time and therefore the rate of spread is affected by the fineness of the fuel material. As such, flames spread more readily through finer, less dense fuels which are more easily ignited by a passing flame, such as those often found in wildland fuel beds.

Experiments through discrete fuel elements have been accomplished in either horizontal or inclined configurations. Vogel and Williams were the first to employ vertical wooden matchsticks of different lengths and spacings to model horizontal fire propagation along fuel elements. They determined required conditions for flame spread as well as presented a model for the forward movement of the fire [20]. Figure 3.1 shows their experimental apparatus. A theory was developed using a constant ignition temperature and a flame stand-off distance profile from a previous study of steadily-burning cellulose cylinders for the ignition time, propagation rate, burning time, char angles and downward propagation rate between matchsticks [22]. The close agreement between theory and experiments lead to the conclusion that

convective effects are the primary controlling factor in flame propagation at a matchstick-size scale.

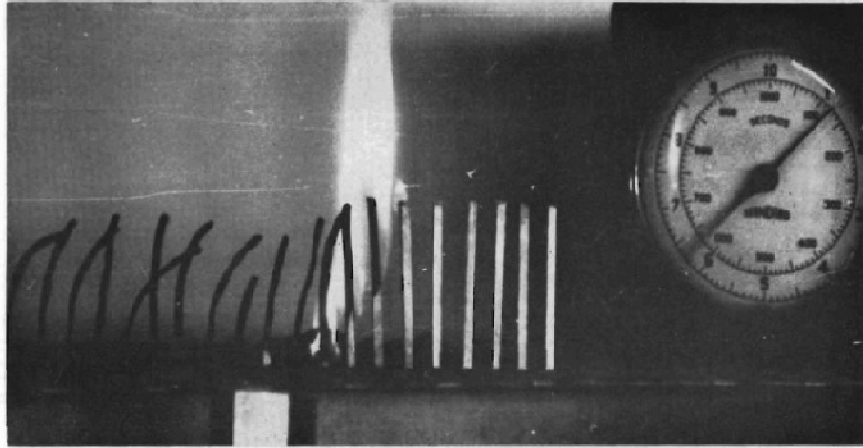


Figure 3.1 Flame propagation along a linear matchstick array from Vogel and Williams [20].

Emmons and Shen utilized paper arrays to model flame spread in their experiments [23]. Figure 3.2 shows a diagram of their experimental apparatus. Measurement were taken of the rate of fire spread through horizontal paper strips placed on their edge, separated by different spacings. It was found that the ignition times observed represented several different burning modes and that steady burning occurs at two different speeds. However, attempts to find a more complete theory failed because there was no overall narrowing of the mechanism responsible for in that couple geometrical configuration.

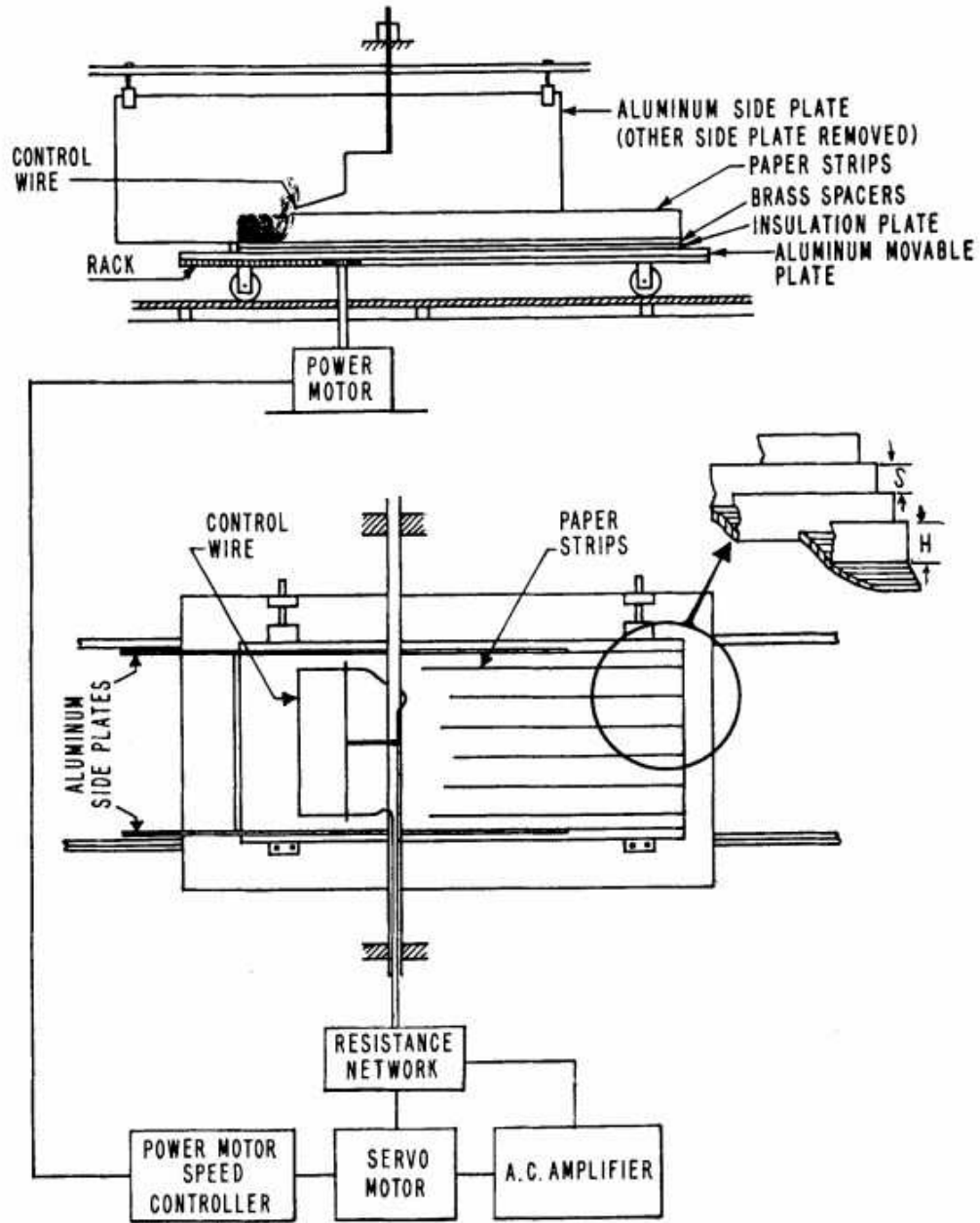


Figure 3.2 Features of the fire spread experimental apparatus used by Emmons and Shen between horizontal strips of paper [23].

Prahl and Tien continued work on flame propagation between single rows of vertically-oriented matchsticks and in rows of continuous paper strips, now adding an imposed ambient velocity from a wind tunnel [24]. The analysis attempted to extend

the previous work of Vogel and Williams by including additional effects of forced convection in the flame spread direction. Figures 3.2 and 3.3 indicate the details of their experimental set up. Based on a combination of elementary theoretical considerations and empiricism, correlations between flame propagation, wind speed, matchstick or paperstrip spacing and fuel height were developed and verified.

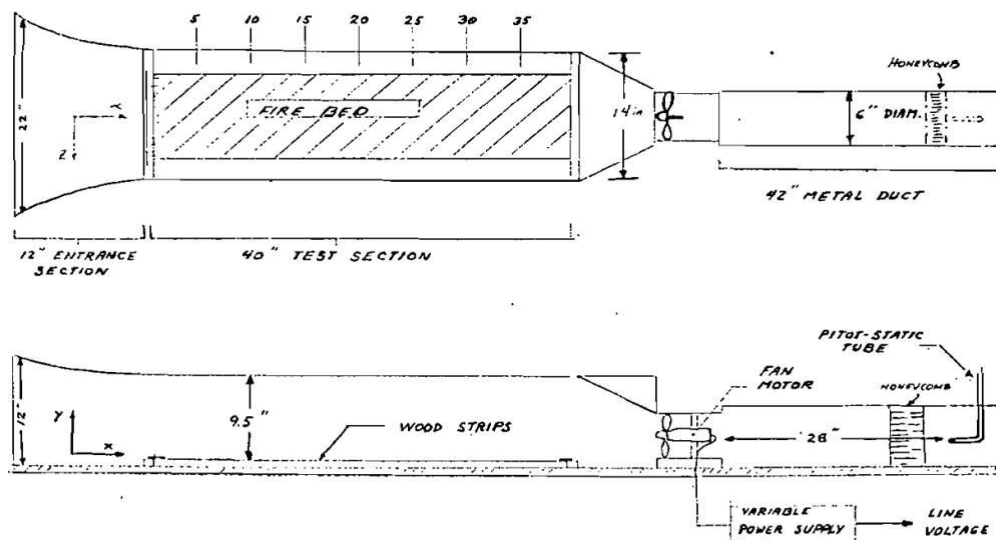


Figure 3.3 Details of the wind tunnel and firebed used by Prahl and Tien (the wind blows from the right fan to the left fuel bed) [24].

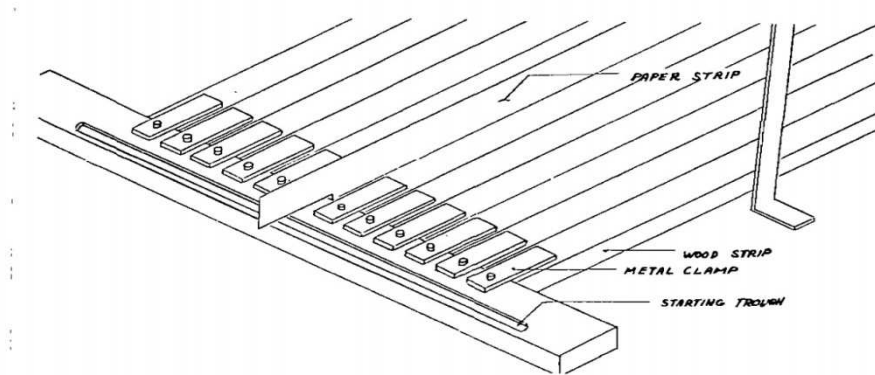


Figure 3.4 Details of firebed used by Prahl and Tien (paper strips clamped down at both end of the fuel bed) [24].

Experiments expanding on horizontal matchstick arrays by Hwang and Xie [25] added the influence of a sloped configuration, with more experiments on paper arrays in similar but larger configurations performed by Emori et al. [26], Weise and Biging have also combined some buoyancy effects into the experimental and theoretical aspects of fire spread through discrete fuel materials [27].

Of all previous studies on arrays of fuels, only one has been conducted on a vertical array. Gollner et al. performed experiments on vertical arrays of horizontally-protruding matchsticks to explore the behavior of upward flame spread over discrete fuels in the laboratory [2]. Figure 3.5 shows the rapid flame spread observed for loosely-packed arrays of matchsticks in their experiments. When the spacing between fuel elements was increased, the flame spread rate was increased due to increased convective heat fluxes from the heated, buoyant flow. Unlike propagation through horizontal arrays, where a steady state is often reached, flame spread through vertical arrays of matchsticks is driven by buoyancy, which results in an accelerating

rate of flame spread. A theory for flame spread rates, burnout times and burning rates was developed for flame spread through a single vertical row of sticks.

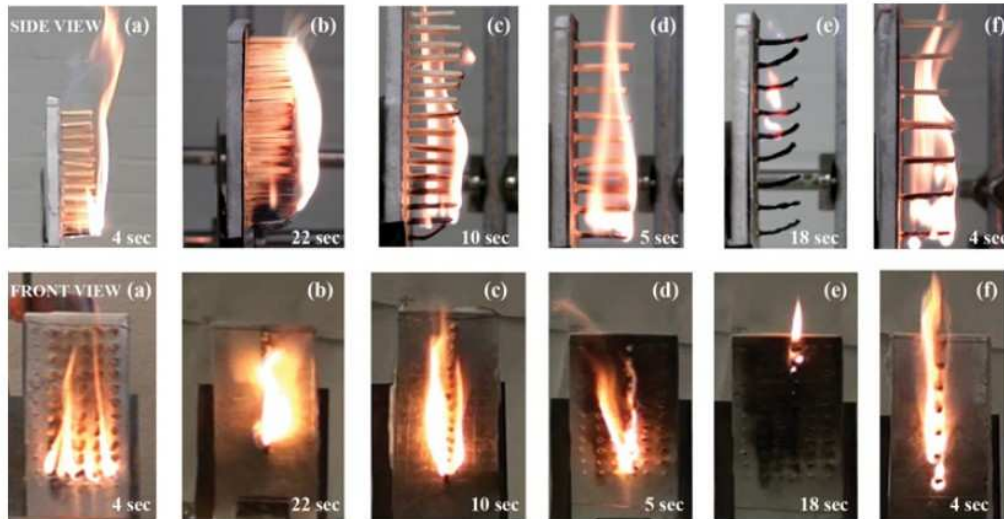


Figure 3.5 Side (top) and front (bottom) video showing the fire behavior observed during experiments. (a)  $S=0.8$  cm array, flame residing on face of matchstick tips; (b)  $S=0.0$  cm single row, flame spreading up matchsticks; (c)  $S=0.6$  cm single row, flame spreading up matchsticks; (d)  $S=0.8$  cm single row, flame spreading up matchsticks; (e)  $S=0.8$  cm single row, matches burning out and bending upward; and (f)  $S=1.4$  cm single row, flame spreading up matchsticks. Note: (b)–(f) are single-column experiments, but holes left from arrays in the metal backing are seen in some of the front images [2].  $S$  indicates the spacing between matchsticks.

### 3.2 Flame Propagation along Cable Trays

Practically, matchsticks arrays and other discrete fuel configurations present similar features to flame spread through cable trays and some wildland fuels. Insulation on electronic cables can provide a considerable density of flammable material when these cables are arranged in large wire trays, such as those found in nuclear power plants and telephone-switching buildings. In fires in cable trays, a small fire started on a lower wire tray will ignite wires above and then spread both vertically and horizontally through the trays. In theory, scale modeling using fuel arrays may assist in the process of designing these trays so that flame spread is limited and maximum heat-release rates of cable trays are reduced.

Hunter, [28] developed an early model to describe flame propagation through horizontal insulated cables and cable trays which were exposed to a fire plume, based on tests performed by Klamerus. The model included limited-oxygen effects by assuming that if the oxygen concentration is not insufficient for ignition, the gas also can accumulate elsewhere and burn later. Ignition delay times and attainable mass fluxes of flammable gases generated by the cable tray were predicted. The delay time increased when the outer radius of the shell of the cable increased, in another words, additional coatings extend the ignition delay time for cables. Longitudinal heat flow was considered as a key factor to prevent direct ignition of single-conductor cables in the cool plumes encountered over cable-tray fires. Figure 3.6 gives a demonstration of Klamerus' tests [28].

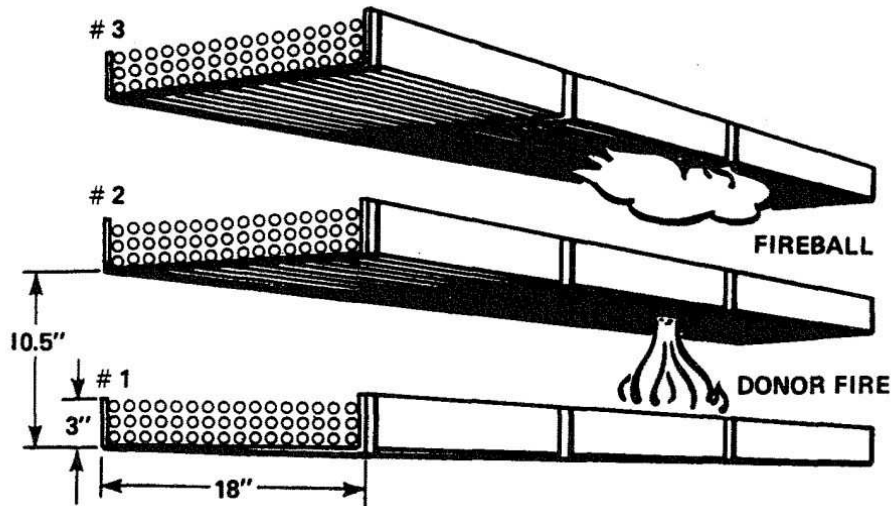


Figure 3.6: Upward fire spread in a stack of horizontal open-bottom trays filled with cables [28].

Alvares and Fernandez-Pello developed an analysis techniques to predict the characteristics of an actual power and communication cable fire, which occurred on 8 May 1988, in Hinsdale, IL [29]. The characteristic parameters included the fuel burning rate, heat-release rate, smokes and HCL generation, growth of the smoke layer, smoke and HCL concentration in the layer, and smoke detector and sprinkler activation times. The analysis presented a simple, alternative way to estimate the development of the fire.

## Chapter 4: Experimental Approach

### 4.1 Method Summary

While Gollner et al.'s previous study provided significant insights into the problem of flame propagation through a single row discrete fuels, it was unable to quantify the effect of wide arrays of discrete objects, where flame spread occurs in two dimensions and is often limited by the high density of available fuel and interactions between fuel elements. In this study, previous work is extended by performing experiments on wide arrays of birch dowels with different spacings. Flame spread occurs both upward through the array and horizontally between columns of dowels as the spacing decreases. While rates of upward flame spread along the center column are well-predicted through the low density arrays, experiments are found to propagate upward significantly slower through the higher density arrays than predicted. This work will document and attempt to describe these effects, with planned work in the future focused on quantitatively predicting these effects.

In this study, an array of wooden dowels were inserted into aluminum plates with different spacings of 0.75, 0.875, 1.0, and 1.5 cm between dowels. Wooden birch dowels with a diameter of 0.32 cm were cut to the length of 3.18 cm and then sealed in an airtight plastic bag until just before experiments, where they were exposed to the laboratory environment. Temperature and humidity measurements

were taken during the experiments and varied between 73°-74°F and 44-46% relative humidity.

To prevent effects of the moisture content of the wood from affecting results, tests were performed at different spacings on different days, multiple times and no variation with different ambient conditions was found.

#### 4.2 Experimental Setup

Figure 4.1 shows an example of the experimental apparatus used in the laboratory along with the configuration for four different spacings. The arrays of wooden dowels were inserted into pre-drilled aluminum plates which are also shown in Figure 4.2. The aluminum plate is a rectangle, with a length of 25.4 cm, width of 20.3 cm and a thickness of 0.5 cm (with an exception being the 1.0 cm spacing plate, where the thickness is just 0.2 cm). The plates were painted black with high-temperature matte paint and also provided clear spaces both below the array of dowels and on the sides in order to reduce the effects of entrainment at the edges of the plate from influencing test results. The aluminum plate was mounted atop a drip pan used to collect any material that may drop during burning. Both were placed atop a load cell to measure the mass of the experiment over time. The load cell was an AND GF-6100, with a measuring range from 0.5 to 1600±0.01 g. The load cell is connected to a computer, reading the mass data 1.7 times per second during the tests. Figure 4.3 gives the appearance of the entire apparatus before a test.

The apparatus was placed below a fume hood to vent the products of combustion and curtains were placed around the far outer edge of the setup to reduce

The apparatus was placed below a fume hood to vent the products of combustion and curtains were placed around the far outer edge of the setup to reduce flow effects from the laboratory from influencing the experiment. The hood was installed 115 cm above the worktable, with a dimension of 92 cm in length and 50.5 cm in width. The curtain was draped around the hood, with only one side open for the operation of experiments.

Two cameras were used in the experiment. One was Sony, high-definition camcorder, recording at 60 frames per second (fps) capturing a wide-angle front view of the entire apparatus, including the spread and flame heights. Another was a Casio EXX-H, high speed camcorder, recording at 300 fps which was focused close up at an angle to burning matchsticks.

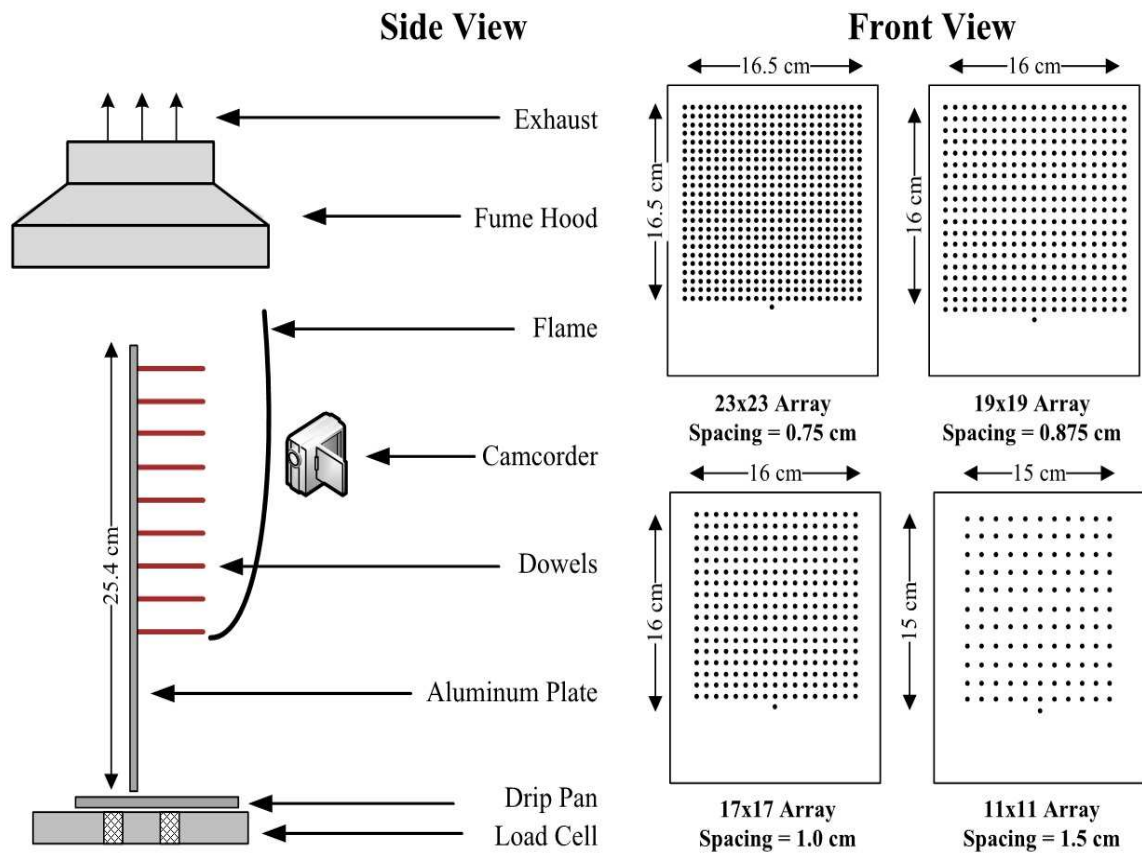


Figure 4.1: Experimental setup (left) and aluminum plates used to hold array of wooden dowels (right).

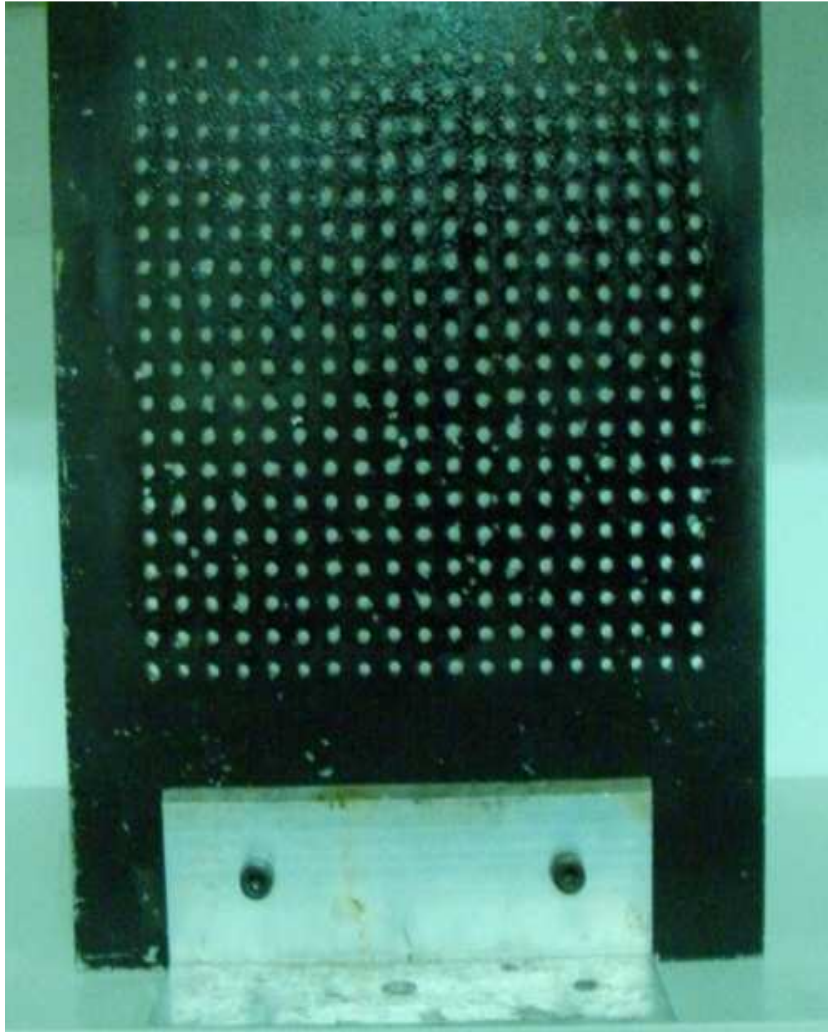


Figure 4.2 Pre-drilled aluminum plate with spacing of 0.875 cm

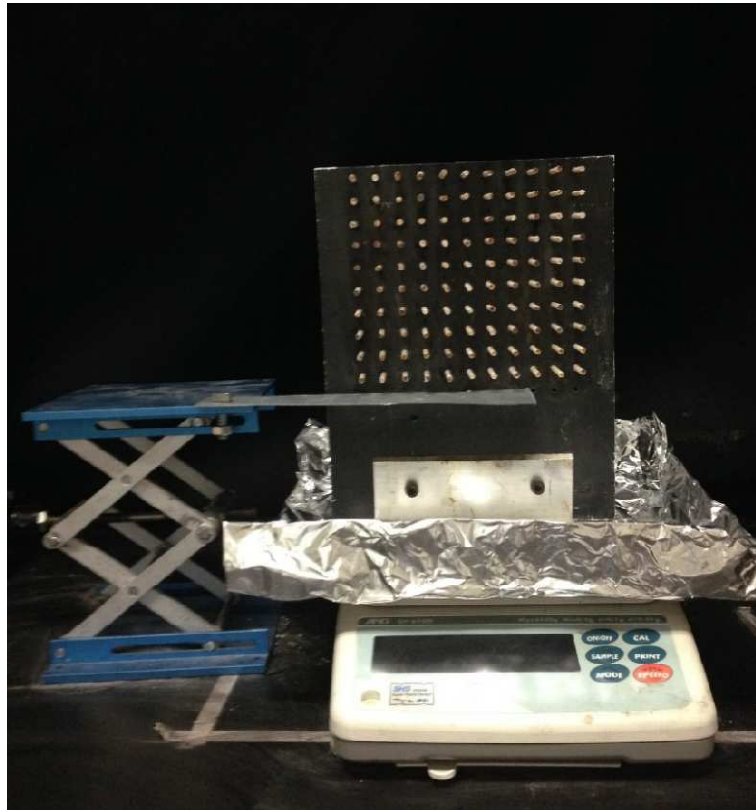


Figure 4.3 Experimental apparatus used with a 1.0 cm spacing plate

### 4.3 Test Specimens

The test specimens are commercially available birch wooden dowels of 0.32 cm diameter. The wooden dowels were cut into 3.18 cm long before each test. This

length was chosen because the top of the wooden dowels were far enough from the pre-drilled aluminate plate to avoid a regime of pure wall burning, while also not being so far that they “curled” toward one another during burning.

Table 4.1: Experimental configurations tested, where  $S/d$  is the ratio of the spacing to diameter of wooden dowels.

<b>Spacing (cm)</b>	<b>Dowel Diameter</b>	<b><math>S/d</math> Ratio</b>
1.5	0.32	4.72
1.0	0.32	3.15
0.875	0.32	2.73
0.75	0.32	2.36

#### 4.4 Experimental Procedure

Wooden dowels were first cut into 3.18 cm long segments, using a band saw. The 3.18 cm matchsticks were sealed in an airtight plastic bag until just before the tests. All the wooden dowels were then inserted into pre-drilled aluminum plates with different spacings, leaving  $L = 2.68$  cm of wood exposed lengthwise, (with an exception being the 1.0 cm spacing plate, where the thickness of the plate was just 0.2 cm, due to availability of material for machining). Additional matchsticks parameters are provided in Table 4.2, with  $w$  the number of columns and  $n$  the number of rows,  $M_i$  the initial total mass of matchsticks and  $A_i$  the total exposed area on the surfaces of the matchsticks.

Experiments were started by igniting one dowel placed below the center or the left-most column of the bottom row. This dowel was ignited with a standard lighter

while a metal plate was held in place above it to prevent ignition or preheating of sticks above. The experimental time began once the metal plate was removed.

Table 4.2: Experimental setup and initial conditions

<b>Spacing <math>S</math> (cm)</b>	<b>Columns <math>w</math></b>	<b>Rows <math>n</math></b>	<b>Initial Mass <math>M_i</math> (g)</b>	<b>Surface Area <math>A_i</math> (cm<sup>2</sup>)</b>
1.5	11	10	11.85	305
1.0	17	16	21.88	837
0.875	19	18	36.83	949
0.75	23	22	54.50	1403
0.75	23	2	4.95	127
0.75	23	3	7.43	191
0.75	23	4	9.91	255
0.75	23	5	12.39	319
0.75	23	6	14.96	383
0.75	23	7	17.34	447
0.75	23	8	19.81	511
0.875	19	2	4.09	105
0.875	19	3	6.14	158
0.875	19	4	8.19	211
0.875	19	5	10.23	264
0.875	19	6	12.28	316
0.875	19	7	14.32	369
0.875	19	8	16.37	421

#### 4.5 Analysis

For each test, data was collected on the mass-loss rate of the entire array, ignition and burnout times of the individual matchstick and flame height of the entire array. Masses measured by the load cell were converted into mass-loss rate by taking the derivative of polynomial fit to the mass lost. Ignition and burnout time were carefully derived by manually stepping frame by frame through a 300 fps recording of the experiments angled at a  $45^\circ$  angle to the front of the array. Ignition was distinguished by observed blacking of at least 50% of the matchstick being observed, while burnout time was indicated by no flame remaining close to the matchstick in question. Observations of a matchstick require care due to flames flicking around the region in question, however observation were often obscured by 5 frames (0.1 second), well with other errors encountered in the experiment. Flame height were found using a technique on front video similar to previously described technique.

The spread of flames through the matchsticks arrays was recorded by a front-facing Sony, high-definition camcorder, recording at 60 frames per second (fps) capturing a wide-angle front view of the entire apparatus, including spread and flame heights. In experiments along single matchsticks by Gollner et al. [2], ignition was recorded with a side-facing camera, this was not doable in present tests because the dense columns of matchsticks obstructing the view. To overcome this, a high speed camcorder, Casio EXX-H, was used to observe the experiments at 300 fps which was focused close up at an angle to burning matchsticks. To get the best observation of igniting matchsticks between flames, the high speed camera was placed at an angle slightly off center line of the plate. In order to track the spread process of the flame

spread, the high speed video was carefully reviewed, by analyzing the footage, frame by frame after tests. This method is the same one as to determine the ignition of matchsticks in Gollner et al.'s previous study, and is only useful for these small scales experiments because flames are not large and bright enough to obscure a view of pyrolyzing from a side view camera. Ignition was defined as the point where 50% of the matchsticks had blackened and burnout was defined as the point when flame adjacent to the burning matchsticks couldn't be observed in the video. To get the mass changing information, a load cell is connected to a computer, reading the mass data 1.7 times per second during the tests.

## Chapter 5: Experimental Results

### 5.1 Physical Observation

After removing the metal plate separating the first ignited matchstick from the array, flames spread above the ignited matchstick impinging on the matchstick vertically above and started heating. Flames from the center bottom matchstick pass on to the matchsticks above them, giving heat to them and leading to a faster spread process that ignites the whole column or array and burns until all flammable gases have been consumed.

In the widest spacing, 1.5 cm, the flame spreads just along the center column of the matchsticks without igniting sticks to either side, as shown in Figure 5.1, similar to previous experiments by Gollner et al. [2]. As the spacing decreases, up to 1.0 cm, the flame primarily spreads along the center column, however towards the top row some horizontal spread occurs, with ignition of matchsticks in adjacent vertical columns, shown in Figure 5.2. In 0.875 cm and 0.75 cm spacings, which are shown in Figure 5.3 and 5.4, flame spread occurs both vertically and horizontally. The rate of upward spread was noticeably slower than in the loosely-packed arrays. White smoke was also observed, indicating some position of the tests were in an under-ventilation condition.

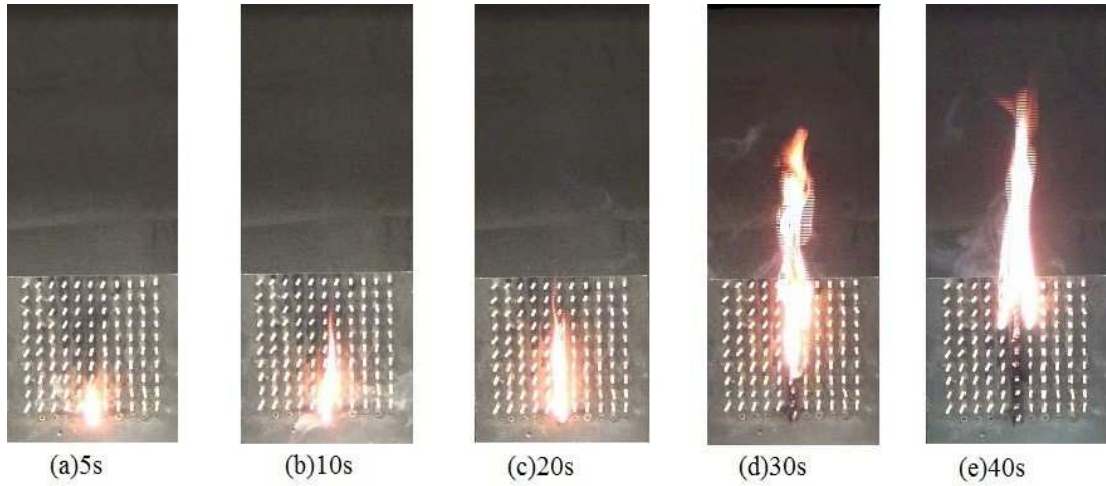


Figure 5.1 Front video showing a time-lapse of the behavior of experiments with a spacing of 1.5 cm. Note only the center row of matchsticks ignite during the spread process

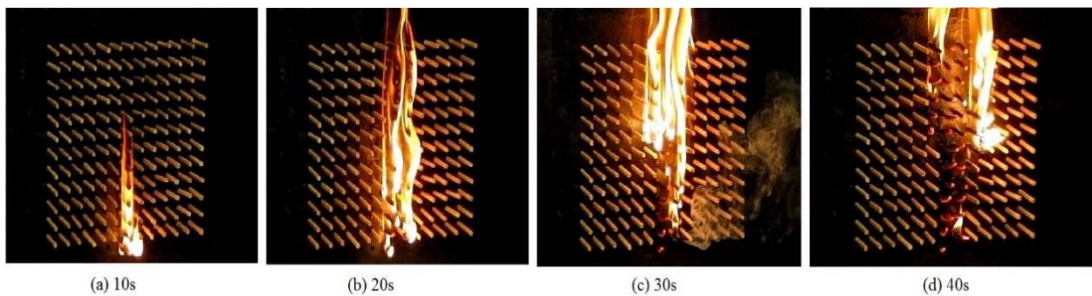


Figure 5.2 Side video showing a time-lapse of the behavior of experiments with a spacing of 1.0 cm. Note that a majority of flame spread occur in the vertical direction, however some wooden dowels to the left and right of the center column begin to ignite.

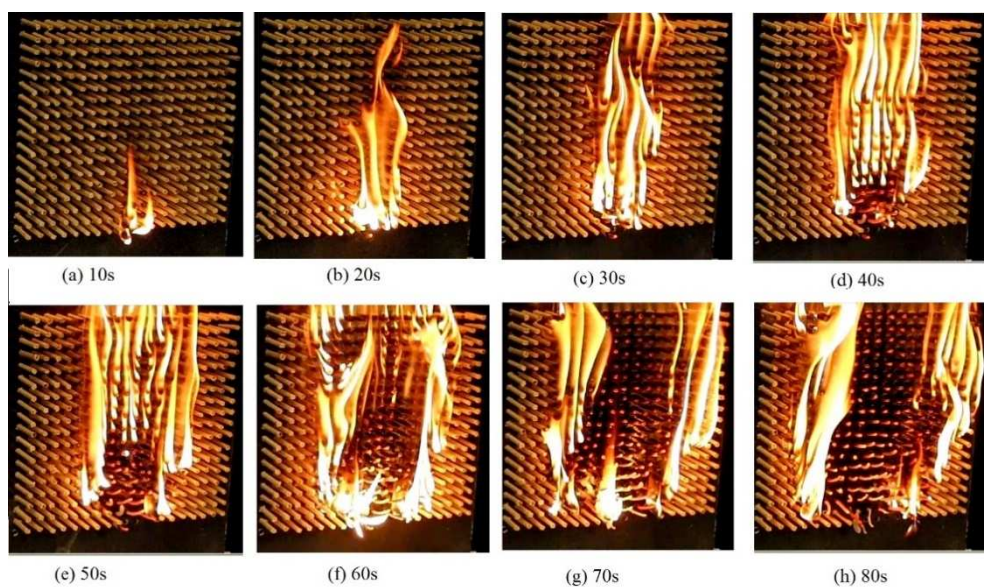


Figure 5.3 Side video showing a time-lapse of the behavior of experiments with a spacing of 0.875 cm. Note that from the base of the experiments, flame spread immediately starts to spread horizontally, eventually involving the whole array.

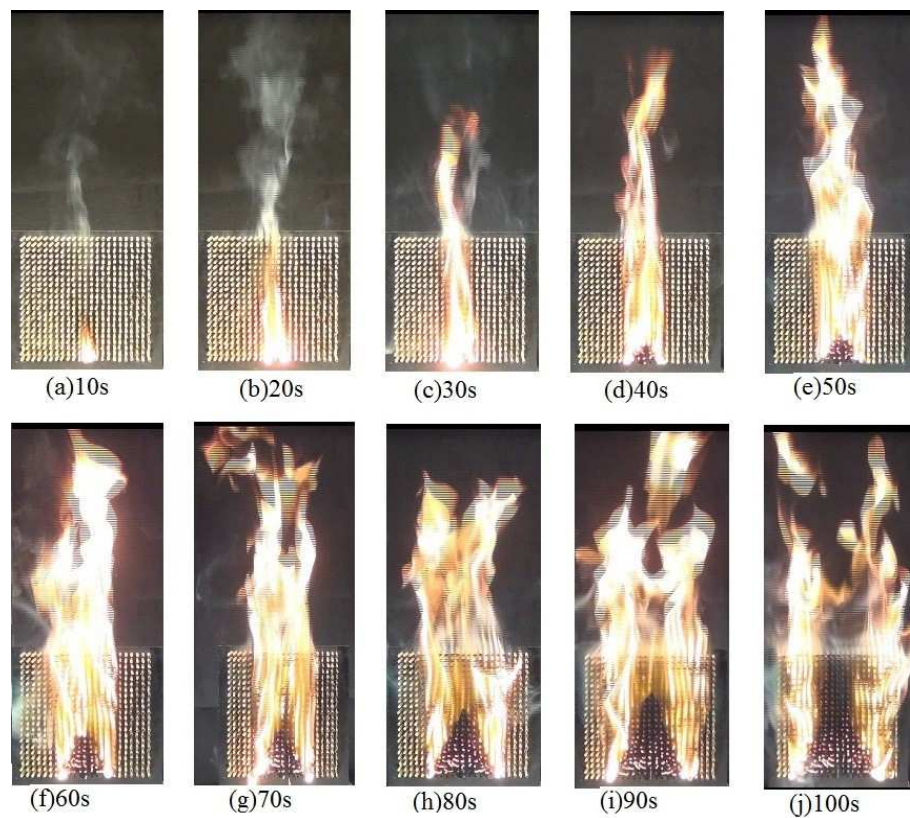


Figure 5.4 Front video showing a time-lapse of the behavior of experiments with a spacing of 0.75 cm. Note that flame spread, from the base, occur both vertically and horizontally, eventually involving entire array.

## 5.2 Vertical Flame Spread

### 5.2.1 Experimental Results

To follow the flame spread along matchsticks, a high speed camera was placed at an angle about  $45^\circ$  off the center of the experiment set up. This angle was chosen to overcome the flame obscuration of pyrolyzing fuel. Pyrolysis front,  $x_p$  was defined as the vertical flame spread over matchsticks. Ignition was defined as at a time when a 50% blackened matchstick was observed and determined by analyzing video footage, frame-by-frame. The method is same to the determination of pyrolysis of Gollner et al. [2] on the single row of matchstick flame spread study. Measurements from each test in each spacing were averaged at each time step. Although blacking is not the actual beginning of ignition, it gave the most approximate way that could indicate the ignition time in different spacings experiments. Figure 5.5 shows the progression of the pyrolysis front.

Models for vertical flame spread predict power-law dependencies between the pyrolysis front and time of the form  $x_p \sim t^a$  because of the influence of buoyancy, which has been reviewed by Fernandez-Pello and Hirano [30] and verified for use in matchstick arrays by Gollner et al. [2]. The power law fit was applied to fit ignition time versus pyrolysis front, which shown in Figure 5.5. In the 1.5 cm spacing experiment, the flame experienced a linear propagation with time, while other spacings fit a power-laws with the exponent from 1.4 to 1.6. With increasing spacing between each matchstick, flames more readily directly impinge on the lower surface of the matchstick above, leading to an increase in heating and shorter time for ignition.

The velocity of buoyant, hot gasses also increases as height increases above the first ignited matchsticks, increasing the heat-transfer coefficient and therefore decreasing ignition times and thus increasing the flame spread rate.

Note that for the densest-spaced data, 0.75 cm spacings there is a sharp increase in the flame spread rate near 70 seconds. While the other tests appear to have experienced a more uniform acceleration, the change in this dense array test is most likely due to further availability of oxygen as the flames spread toward the end of the array, where it is open to the atmosphere. Further discussion of this effect and related experiments on horizontal propagation are shown later.

### 5.2.2 Analysis

Vogel and Williams [20] developed a theory, calculating ignition times corresponded with flame jump times in their study of horizontal arrays of matchsticks. In the present experiments, ignition times do not equal to flame jump times in the horizontal configuration because when heights increases, buoyant hot gases flow faster, increasing heating rates and shortening ignition times. For example, ignition times increase as  $t^{1.4}$  to  $t^{1.6}$  when the spacings are smaller than 1.5 cm. Ignition times in horizontal arrays were achieved only by use of a transient heat-conduction equation, while in the present experiments convection heat transfer may be more appropriate to estimate the ignition times and so explain relevant heat transfer processes occurring.

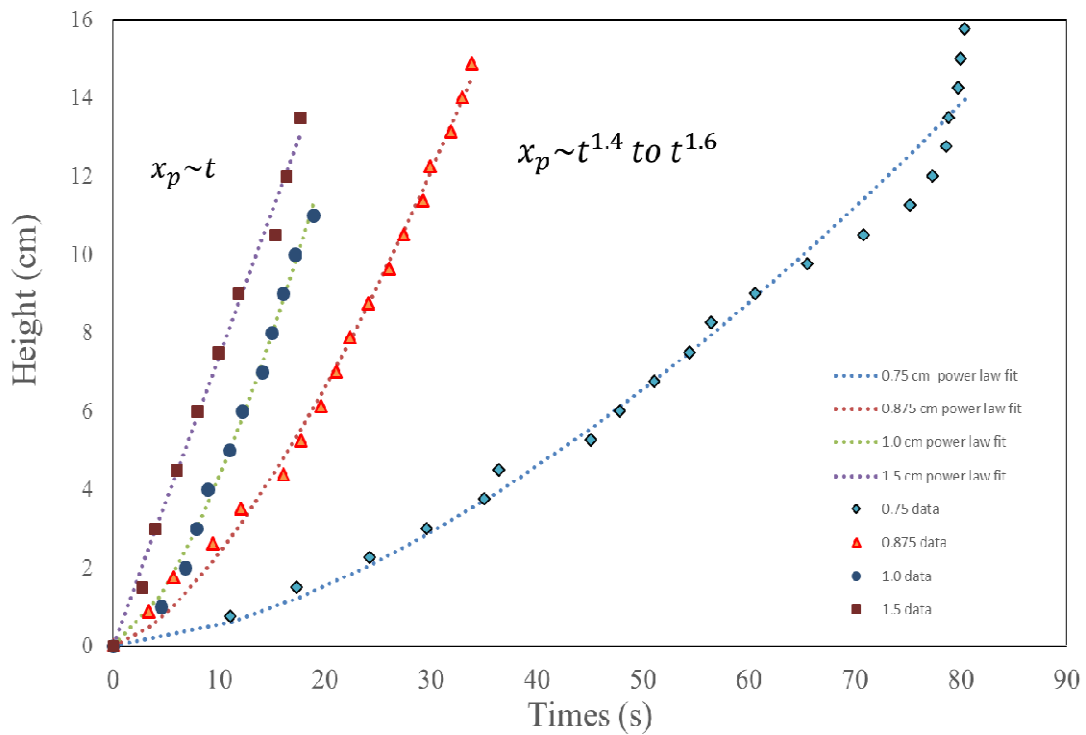


Figure 5.5 Progression of the pyrolysis front. Symbols indicates the location of the pyrolysis front observed from the high speed video and dashed lines indicate power-law fit to this data.

As shown in Equation 2.3,  $t_{ig} = t_{py} + t_{mix} + t_{chem}$ , the ignition time for a solid material contains chemical, mixing and pyrolysis process, however the chemical time for ignition can be estimated and is on the order of  $10^{-4}$  s, which is very small and can be negligible in this whole process. To get an approximate estimate of the mixing time,  $t_{mix}$  can be calculated by assuming a laminar boundary layer exists over the surface of the matchstick. The matchstick could be treated as a cylinder, where  $\delta_{BL} \sim d/\sqrt{Re_d}$ , and the Reynolds number  $Re_d$  was assumed to be between 50-500 for this study depending on height. The boundary layer thickness within which the diffusion flame occurs can be estimated as  $\delta_{BL} \approx \sqrt{\alpha_m t_{mix}}$ , where  $\alpha_m$  is the mass diffusivity of gas. Then the mixing time can be approximated on the order of  $10^{-1}$  second for laminar flow. Therefore it is also much smaller than the pyrolysis time that has been observed.

The ignition time for a thermally thin material can now be expressed as

$$t_p \approx \frac{\rho_s c_{p,s} d (T_p - T_\infty)}{\bar{q}''} , \quad (5.1)$$

where  $\rho_s$  and  $c_{p,s}$  are the material's density and specific heat capacity, which are constant material properties,  $d$  is the thickness of the fuel,  $T_p$  is the pyrolysis temperature of the fuel and is assumed that  $T_p \approx T_{ig}$ ,  $T_\infty$  is the ambient temperature and  $\bar{q}''$  is the average heat flux per unit area given to the unignited matchstick while the flame puff around the surface. Because of the fact that the thickness of the matchstick is less than its thermal penetration depth,  $l_{th} \sim k_s (T_{ig} - T_\infty) / \bar{q}'' \approx 0.1$  mm,

the assumption of thermally thin behavior is reasonable. The average heat flux here can be estimated from correlations for cross flow along a blunt body or laminar convection down a vertical plate.

It is assumed that the heat-transfer is dominated by convection, ignoring radiation effects due to the experiments small size, related to a heat-transfer coefficient,  $h$  which will be determined by a Nusselt number correlation for the different spacings experiment. For a buoyant flow, a Grashof number correlation would typically be used, but when the separation is sufficient where  $S$  is much larger than  $d$ , an upper cylinder will lie in the “fake wake” of the lower cylinder [31]. In the far wake, the details of the size and shape of the lower cylinder are unimportant, therefore the flow can be estimated as cross-flow over a cylinder. The Reynolds number can be assumed by using a forced-flow correlation which can be written as

$$Re_d = \rho_g u_g d / \mu_g , \quad (5.2)$$

where  $\rho_g$  and  $\mu_g$  are the density and viscosity of gas, respectively and  $u_g$  is a buoyant velocity approximated from the height of the matchsticks position  $x$ ,

$$u_g \approx \sqrt{g x} , \quad (5.3)$$

where  $g$  is the gravitational acceleration, and  $x$  can be calculated as

$$x = (S + d) \times n + d , \quad (5.4)$$

where  $n$  is the rows number of the matchstick when the flame reach in the test.

A correlation used here which can describe heat transfer from the flame to individual matchsticks is

$$\overline{Nu}_d = 0.344Re_d^{0.56}, \quad (5.5)$$

where  $\overline{Nu}_d = \overline{h}d/k_g$  is the average Nusselt number of the flow. This correlation for cross-flow over cylinders was used by Gollner et al. [2] to explain heat transfer from vertical flames to single row of matchstick, and predicted ignition time accurately in their study, encouraging its use in present study.

Figure 5.6 shows the calculated pyrolysis front, as a function of time, compared with power-law fits to experimental data shown in Figure 5.5. In the 1.5 cm, 1.0 cm and 0.875 cm tests, the calculated ignition times match a power-law fit to the experimental data well. The flow in these spacings will not only be around the edges of matchsticks, but also touching the bottom and top surfaces, bathing all the surfaces with flame, so the heat transfer correlation for cross-flow over a cylinder closely matches in these looser spacings tests. When the flames get to the higher matchsticks in the tests, buoyancy makes hot gases flow faster, resulting in an increase in heat transfer rates and a similar acceleration in the flame spread rate which corresponds to the observation during the tests. This acceleration may also be caused by an increase in radiative heating, however, the good match when using the convective correlations to explain the heating process reveals that convective, not radiative heat transfer is the dominant mechanism at this small scale.

Unlike other tests, the 0.75 cm test calculated ignition times are much smaller than the experimental data fit line, which means flame spread was much slower than

the theory predicted. This result may be related to the configuration of the matchsticks. In the 0.75 cm experiments, matchsticks are close to each other, occupying much more space than other tests which may block the air entrainment from the environment. This may both block flames from heating above matchsticks as well as reduce the availability of oxygen within the test, reducing flame heights and thus heating and spread rates. A limited-oxygen scenario is further corroborated due to observations of significant white smoke during flame spread and burning in the densest configuration but not others, and also because of a jump in the flame spread rate toward the end of all 0.75 cm spaced tests, signaling increasing availability of oxygen due to ambient air availability on the top of the array.

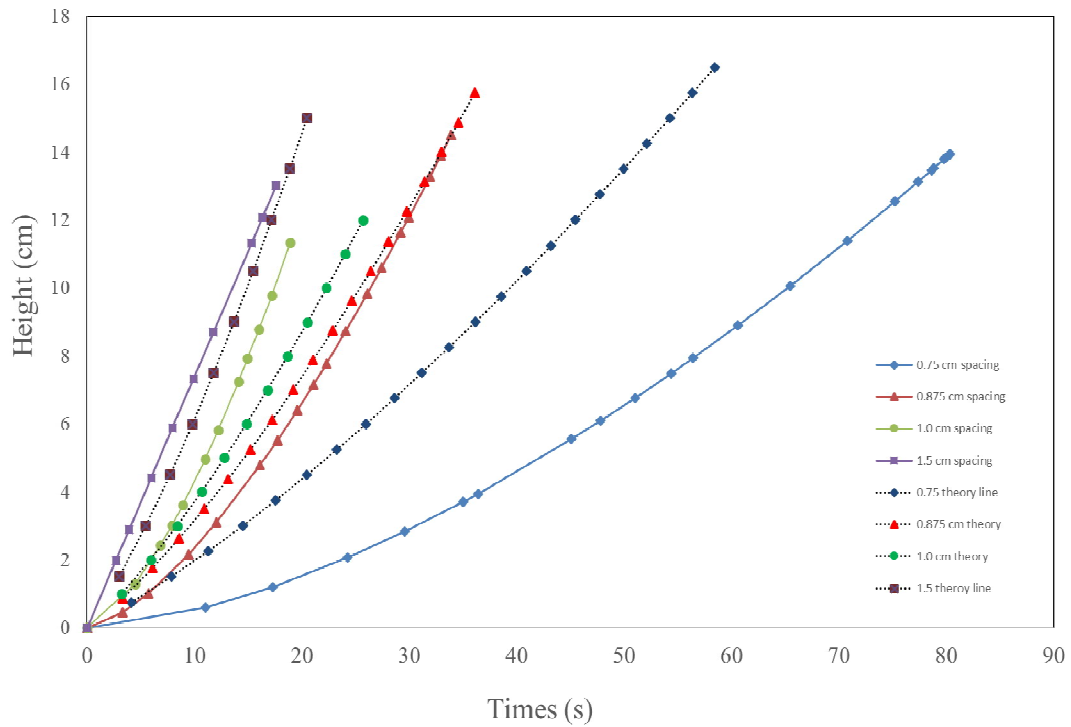


Figure 5.6 Calculated ignition times using convection heat transfer correlations (symbol with dashed line) are compared with power-law fits to experimental data (symbols with solid line).

### 5.3 Burnout Times and Burning Duration Times

#### 5.3.1 Experimental Results

Burnout times throughout the array were observed using the same high speed video technique and defined as the point when there was no flame observed in the video. Figure 5.7 shows the results of center column burnout times as a function of height. The burnout data may be more subject to errors in observations as well as inconsistent processes during the burning of single matchstick and not so clear as the ignition time data. Trends however are still similar to those seen in Figure 5.5.

The burning duration time was defined as the time between the ignition times and the burnout times. Figure 5.8 shows the burning duration times as a function of height for the center column of each test. The average time seems to be constant in each test. Data from 1.5 cm and 1.0 cm experiments are longer than the theory burning duration time; the 0.875 cm case shows two regimes, the first part is from the bottom matchstick to about the ninth row, for which the burning duration times are around the theory line, the second part is from the tenth row to the top matchstick, which has a longer duration times compared to the theory line; the burning duration times in the 0.75 cm tests have smaller values than the theory. From Figure 5.8, a trend indicates that burning duration time will increase with decreasing spacing between each matchstick. There are two possible mechanisms which may affect the burning duration times. In the denser spacing experiments, matchsticks next to each other will limit surface exposure to flames and heating and also limit the outflow of pyrolysis vapors from the wooden dowels. Another contribution, the lack of oxygen

during burning process, may provide a better explanation to match the observations. Because of the fact that matchsticks were so close to each other, it is possible that this configuration limited enough oxygen to be entrained into the flow field to sustain the burning of the matchsticks.

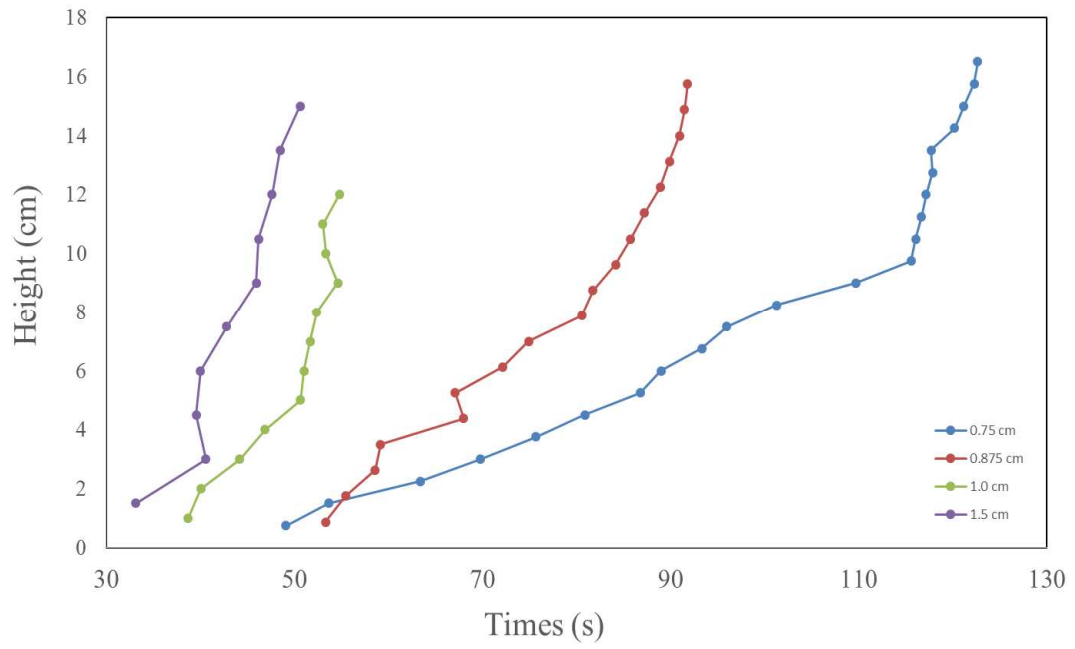


Figure 5.7 Burnout times through the center column of the array

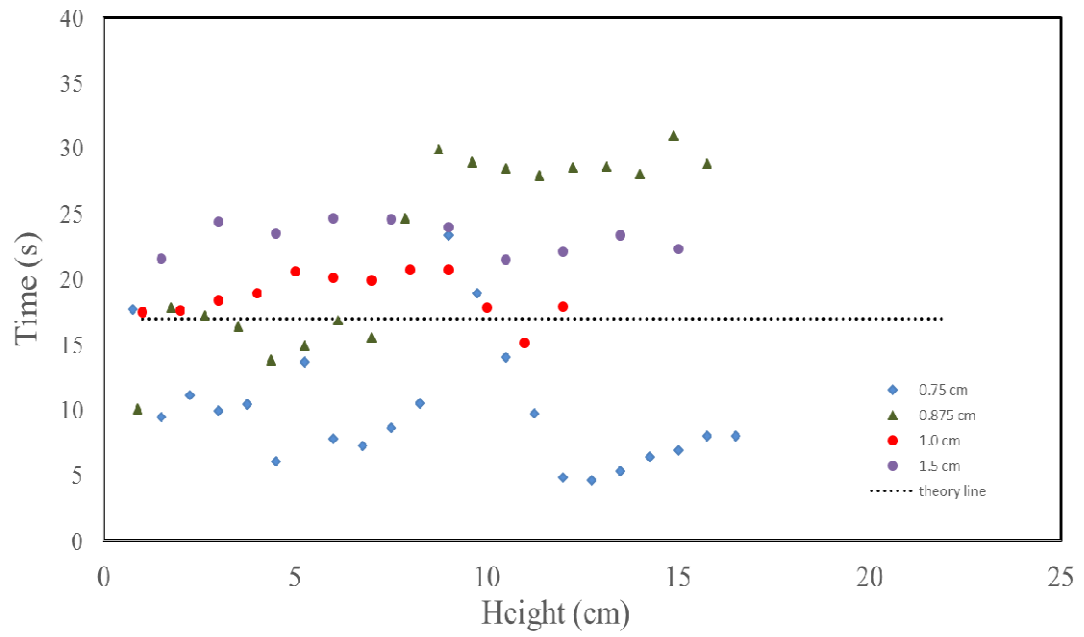


Figure 5.8 Burning duration times. Experimental data are shown by symbols

and predictions are shown as a dashed line.

### 5.3.2 Analysis

From Gollner et al.'s previous study, experiments here should be considered as the case which spacing is large enough so that the matchstick burns as an individual element. The method to analyze the data for burning rate is similar to the analysis of Lee [32]. The theory for a single spherical fuel droplet can be regarded as a cylindrical geometry. Explain To get the mass-loss rate of a horizontal cylinder, a Schvab-Zeldovich formulation with a flame-sheet model and a correlation for flame standoff distance is used. With initial radius  $r_i = d/2$ , the mass loss rate for the cylinder can be written as

$$\dot{m}' = -\frac{d}{dt}(\rho_s \pi r_s^2) = 2\pi r_s \rho_s \frac{dr_s}{dt} = \dot{m}'(r_s), \quad (5.6)$$

where  $\dot{m}'$  is the mass-loss rate per unit length of the cylinder and  $r_s$  is the radius of the cylinder at time  $t$ .

The burning duration time for a cylinder can be calculated as

$$t_b = \int_0^{r_i} \frac{2\pi r_s \rho_s}{\dot{m}'(r_s)} dr_s. \quad (5.7)$$

According to Lee's study,  $\dot{m}'(r_s)$  can be found as

$$\dot{m}'(r_s) = \frac{2\pi k_g}{c_{p,g} \ln(r_f/r_s)} \ln(1+B), \quad (5.8)$$

where  $B$  is the mass transfer number of the fuel,  $B \approx [Y_{O_2, \infty} \Delta H_c - c_{p, \infty} (T_p - T_\infty)] / \Delta H_p$  and integrating Equation 5.7, the burning duration time for a cylinder ( $S \approx \infty$ ) is

$$t_b = \frac{\rho_s c_{p,g} r_i^2 [2 \ln(r_f/r_s) + 1]}{4k_g \ln(1+B)} \quad (5.9)$$

The ratio of flame standoff distance to initial radius in Equation 5.9,  $\ln(r_f/r_i)$  is calculated from the correlation,  $\ln(r_f/r_i) = 0.2(d/2)^{-0.75}$ , with  $d$  in cm, derived from Lee's study [32]. The values of other parameters used to calculate  $t_b$  are presented in Table 5.1. The burning duration time was calculated to be 17.04 seconds. The prediction line is shown as dashed line in Figure 5.8.

Table 5.1: Values of properties used in burning duration time calculations.

	<b>Property</b>	<b>Quantity</b>	<b>Citation</b>
$B$	Mass transfer number	1.75	[20]
$c_{p,g}$	Specific heat of gas	1065 J/kg · K	[20]
$d$	Diameter	$3.2 \times 10^{-3}$ m	
$k_g$	Thermal conductivity of gas	0.06 W/m · K	[20]
$\ln(r_f/r_s)$	Flame to surface radius	0.79	[20]
$\rho_s$	Density of solid	$5 \times 10^{-3}$ m	[2]

## 5.4 Horizontal Flame Spread

### 5.4.1 Horizontal Experimental Results for Full Arrays

As mentioned earlier, in 1.5 cm arrays, horizontal flame spread barely appears. In the 1.0 cm case, horizontal spread doesn't show up until the flame reaches the 7th row above the bottom and only 4 or 5 matchsticks have been ignited in the upper rows. In the 0.875 cm arrays, horizontal spread seems to be faster in the upper rows than the lower rows, so some rows in the center of the array may be heated from both the upper and lower sides. In the 0.75 cm spaced array, flame spread exhibits a 2-D nature, spreading throughout the arrays in a full V-shaped pattern. A plot of horizontal flame spread in full arrays experiments is shown in Figure 5.9 and indicates the linearity of the horizontal flame propagation, which is the same as Prahl and Tien [24] found in their study for horizontal matchstick flame spread under wind-driven conditions. Also in 0.75 cm and 0.875 cm tests, the horizontal spread rates are very close, but the 1.0 cm spacing case shows a faster spread behavior which can also be observed in upward flame spread.

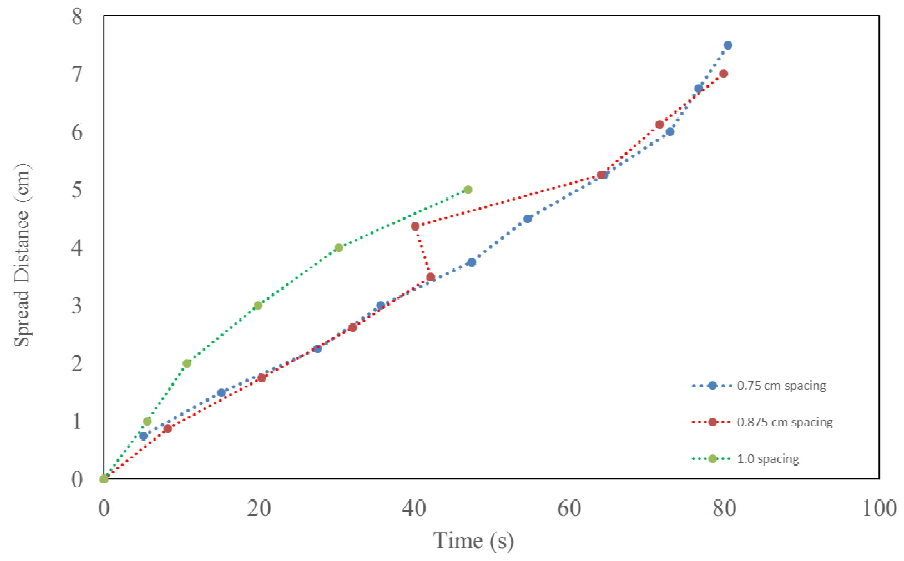


Figure 5.9 Horizontal flames spread in full arrays

#### 5.4.2 Horizontal spread experiments of different rows of matchsticks

To gain more insight into horizontal spread along wooden dowel arrays, tests on different rows of matchsticks were conducted horizontally as shown in Figure 5.10-5.14. In the 1.5 cm and 1.0 cm spacing tests, no matter how many dowels were inserted into the plates, there is no horizontal spread appearing when the left-most dowel in the bottom row were ignited. For the 0.875 cm cases, when there are only two or three rows in the plate, flames only spread to some matchsticks in the upper rows and will not burn all the matchsticks, shown in Figure 5.10 and 5.11. The whole row's horizontal flame spread appears when the row's height increases to become four and larger, shown as Figure 5.12. This indicates that there is some influence of nearby matchsticks on horizontal ignition and spread.

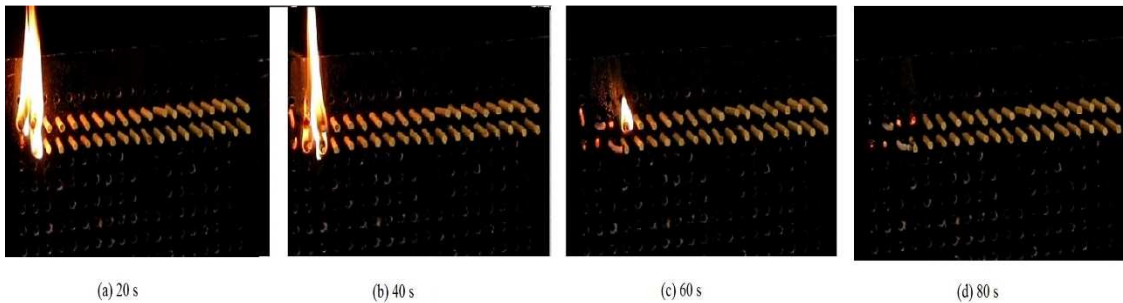


Figure 5.10 No horizontal flame spread behaviors happened with a spacing of 0.875 cm in 2 rows

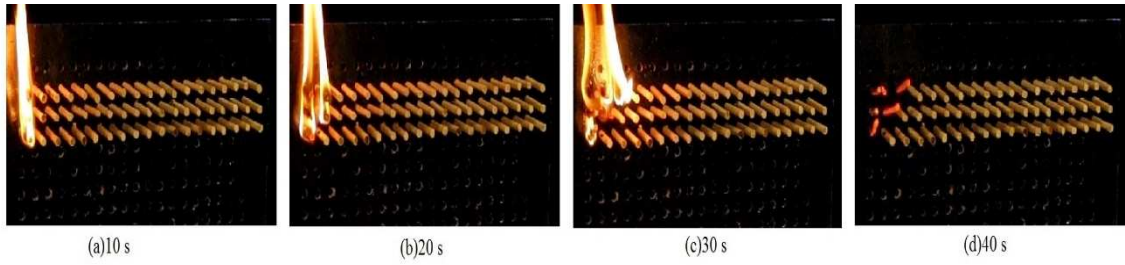


Figure 5.11 No horizontal flame spread behaviors happened with a spacing of 0.875 cm in 3 rows.

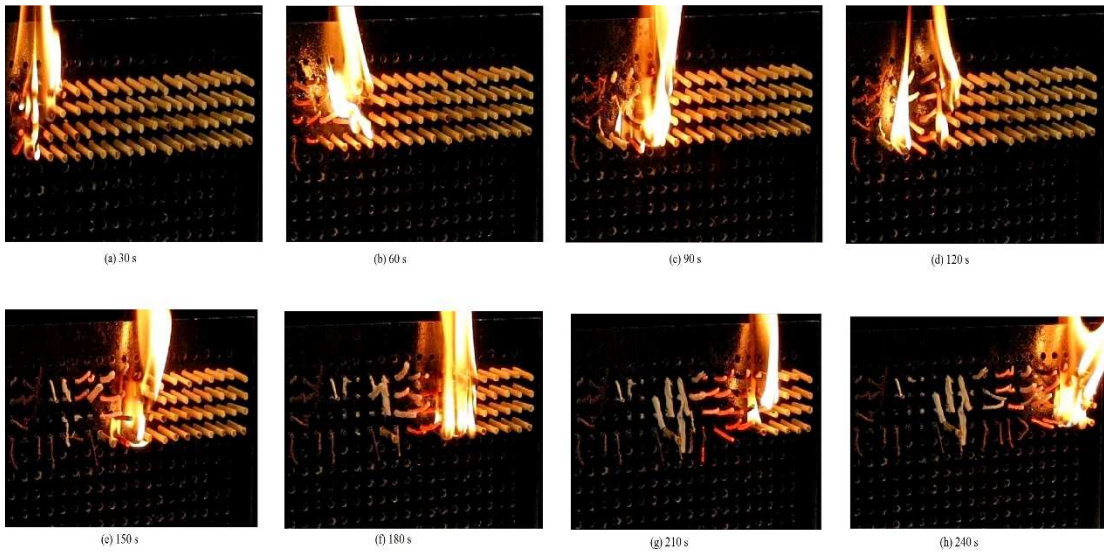


Figure 5.12 Horizontal flame spread behaviors with a spacing of 0.875 cm in 4 rows.

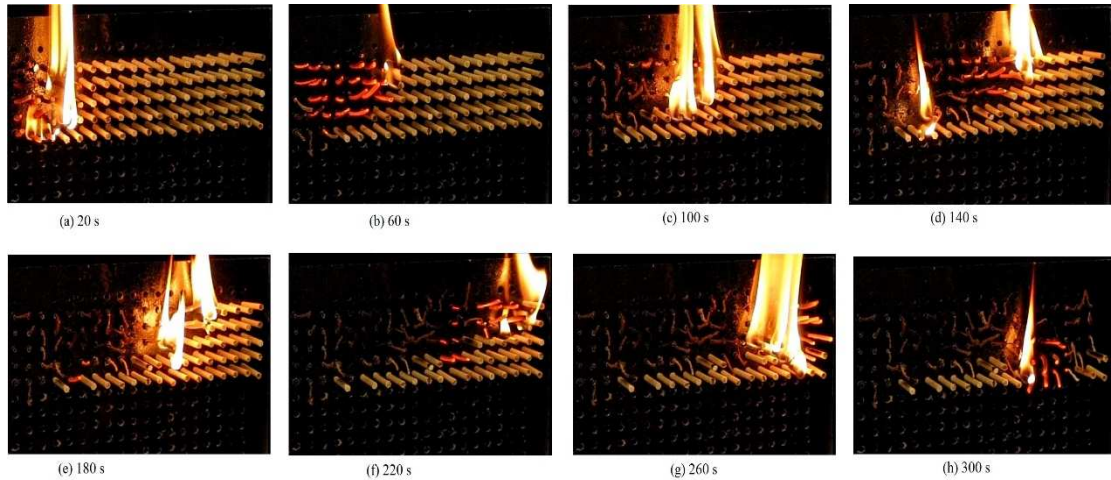


Figure 5.13 Horizontal spread behavior with a spacing of 0.875 cm in 5 rows.

In the 0.875 cm spacing, when there are 5 rows in the plate, flames spread horizontally along the upper rows from left to right, leaving some matchsticks unignited underneath, as shown in Figure 5.13 ((a)-(f)). Then the flame spreads downwards and back to the left, igniting some of the unburnt matchsticks, shown in Figure 5.13 ((g)-(h)). A similar spread behavior also shows up in 7 rows test, shown in Figure 5.14.

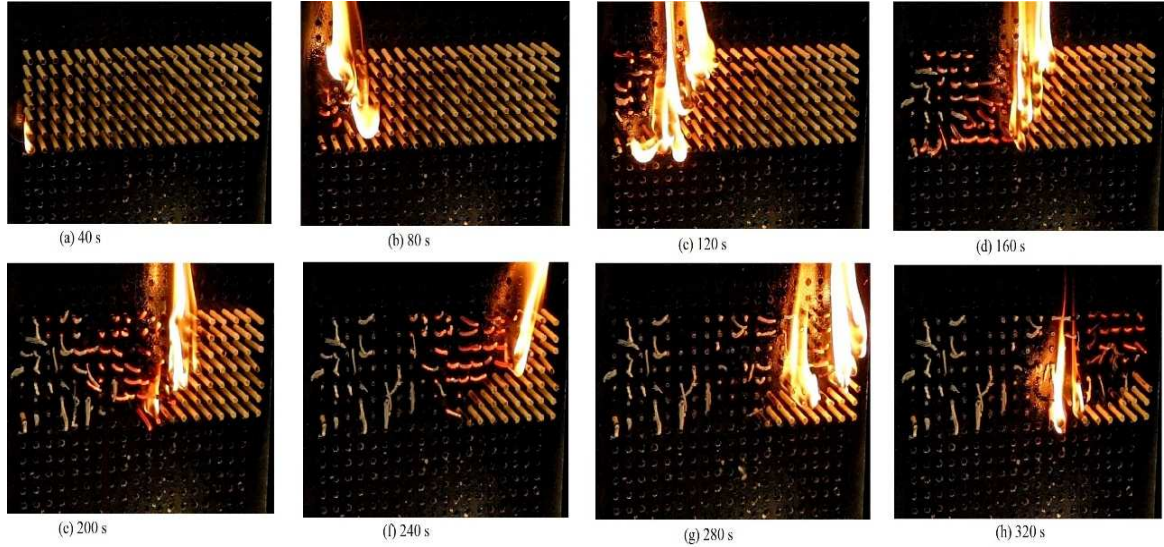


Figure 5.14 Horizontal flame spread behavior with a spacing of 0.875 cm in 7 rows.

### 5.4.3 Analysis

Figure 5.15 and 5.16 show the plots of horizontal flame spread as a function of time. The figures show a linearity of the horizontal propagation, which shows some similarities as depicted in Vogel and William's study [20]. Based on their previous study, ignition time can be expressed as

$$t_i = \frac{\pi k^2}{4\alpha k_g^2} \left( \frac{T_i - T_0}{T^* - T_0} \right)^2 (s - cl^{0.25})^2, \quad (5.10)$$

where  $k$  and  $k_g$  are the thermally conductivity of solid and gas respectively,  $\alpha$  is the thermal diffusivity, which can be calculated by equation  $\alpha = \frac{k}{\rho c_{heat}}$ ,  $T_i$  is the ignition temperature,  $T_0$  is the initial temperature,  $T^*$  denotes the flame temperature,  $s$  is the spacing between matchsticks,  $c$  is a constant, whose value is 0.16 found in Vogel and Williams's research and  $l$  is the length of matchsticks. Table 5.2 gives values of all the parameters in Equation 5.10. It indicates with the row's number increases, the

flame spread time decreases. This may be due to the more probabilities for flame to reach to the fuel in experiments with more rows.

Table 5.2: Values of properties used in ignition time calculations.

	<b>Property</b>	<b>Quantity</b>		<b>Citation</b>
$k$	Thermally conductivity of the solid fuel	$3.8 \times 10^{-4} \frac{cal}{cm} sec \text{ } ^\circ K$		[20]
$k_g$	Thermally conductivity of the gas	$1.2 \times 10^{-4} \frac{cal}{cm} sec \text{ } ^\circ K$		[20]
$T_i$	Ignition temperature	370°C		[20]
$T_0$	Initial temperature	25°C		
$T^*$	Flame temperature	~1500°C		[20]
$c$	Constant	0.15		
$l$	Length of the matchstick	1.0 inch		
$c_{heat}$	Heat capacity	0.36 cal/g		[20]
$s$	The spacing between matchsticks	0.29 inch for 0.75cm case	0.34 inch for 0.875 cm case	

A comparison of the  $t_i$  given in Equation 5.10 with the experimental data on Figure 5.15 and Figure 5.16 appears in Table 5.3 and Table 5.4. Flame jump time  $\Delta t$  is defined as the average time interval between two adjacent matchsticks and calculated as

$$\Delta t = \frac{t}{L/s}, \quad (5.11)$$

where  $t$  is the total propagation time,  $L$  is the distance of the propagation and  $s$  is the spacing between each matchstick.

Table 5.3: Comparison of Theoretical and Experimental Propagation in 0.75 cm case

<b>Row number</b>	<b>s(inch)</b>	<b>Theoretical <math>t_i</math> (sec)</b>	<b>Experiment data <math>\Delta t</math> (sec)</b>
3	0.29	5.5	11.3
4	0.29	5.5	9.8
5	0.29	5.5	9.9
6	0.29	5.5	8.9
7	0.29	5.5	8.2
8	0.29	5.5	7.9

Table 5.4: Comparison of Theoretical and Experimental Propagation in 0.875 cm case

<b>Row number</b>	<b>s(inch)</b>	<b>Theoretical <math>t_i</math> (sec)</b>	<b>Experiment data <math>\Delta t</math> (sec)</b>
4	0.34	10.31	12.44
5	0.34	10.31	12.45
6	0.34	10.31	10.01
7	0.34	10.31	10.49
8	0.34	10.31	8.08

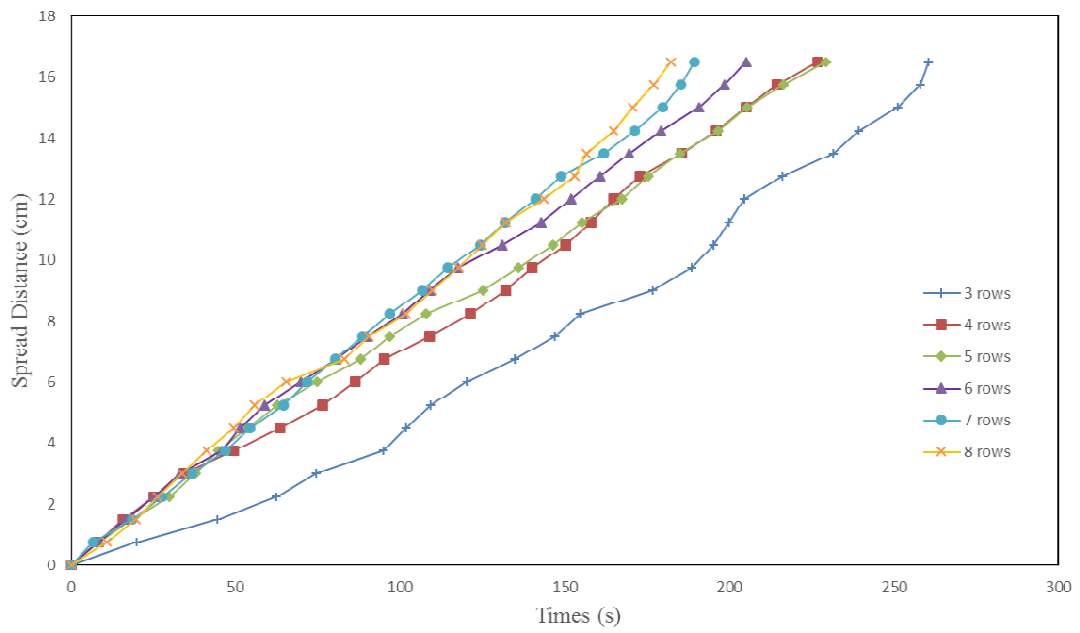


Figure 5.16 Horizontal flame spread with a spacing of 0.75 cm in different rows.

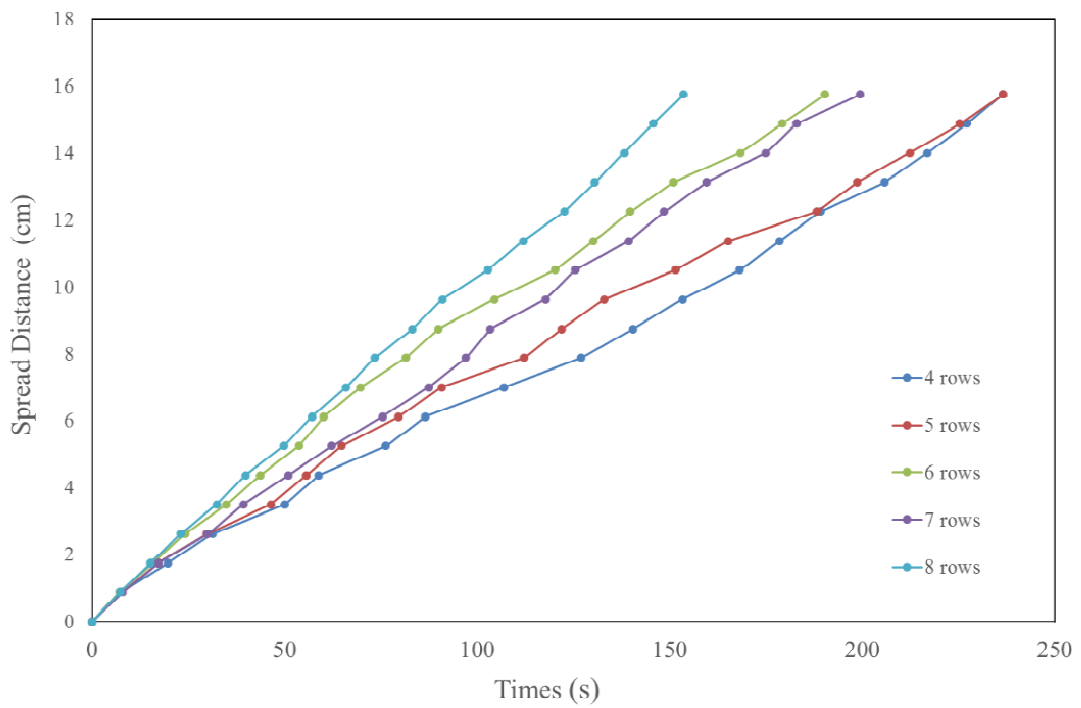


Figure 5.15 Horizontal flame spread with a spacing of 0.875 cm in different rows.

## Chapter 6: Conclusion

Study of full arrays of matchsticks has provided a useful surrogate to explore the flammability of discrete fuels, showing the influence of spacing has on the upward and horizontal flame propagation. The fluid dynamics of the flow field around the matchsticks is regarded as an important part which will have a significant effect on the heat transfer mechanism. Standard heat transfer correlations for observed flow scenarios were adapted to predict ignition times for matchsticks, which revealed the controlling mechanism of convective heat transfer being responsible for ignition at this small scale. Burning duration time rates were predicted using a burning rate theory for a cylindrical geometry. The results indicate a limit to the theory developed through single columns of matchsticks by Gonller et al. [2] and theory from the linear, horizontal arrays of vertically oriented matchsticks by Vogel and Williams [20]. The spacing between each matchstick encourage flame interaction and decrease the fire spread rate due to a lack of available oxygen.

## Appendices

Mass-loss histories were recorded for all spacings, averaged together and plotted here. Figure A-1 shows the mass loss history during the experiments. In the beginning of the tests, all the mass-loss recordings seemed to be the same because only the center columns were ignited. After that, for denser spacing experiments, more and more matchsticks were ignited and more mass was lost. The dashed lines indicate the smoldering phenomenon in the denser experiments. Although there was no flame observed, the mass was still decreasing because of the smoldering. Figure A-1 also indicates the burnout time for each experiment and it is clear that with more matchsticks in place the burnout times becomes longer. The mass-loss rates shown in Figures A-2 increase over time in the region of upward spread and begins to decrease as matchsticks burn out. The dashed lines for denser experiments also shows that smoldering could happen even there was no flame observed from the video. The mass loss rate per unit area for different spacings tests, shown in Figure A-3, was calculated by dividing the mass-loss rates by the area burning during the tests determined by observations of ignition detailed earlier. Plots of the mass-loss rate per number of matchsticks ignited and per total number of matchstick are also shown in A-4 and A-5.

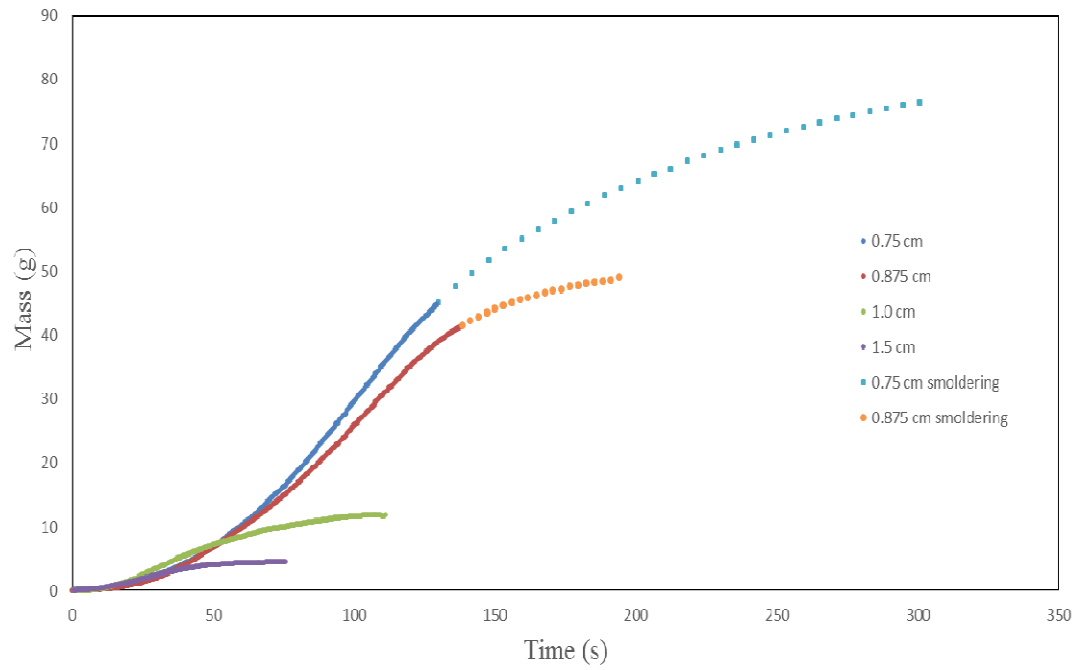


Figure A-1 Mass-loss history during the tests

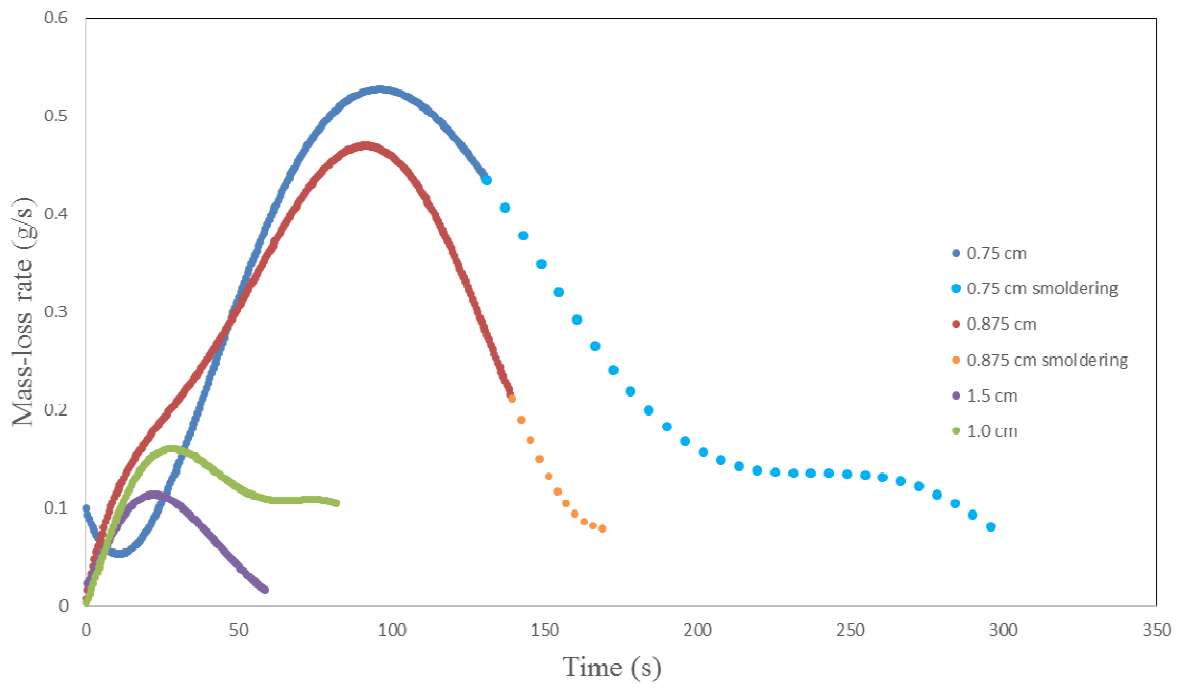


Figure A-2: Mass-loss rate during the tests

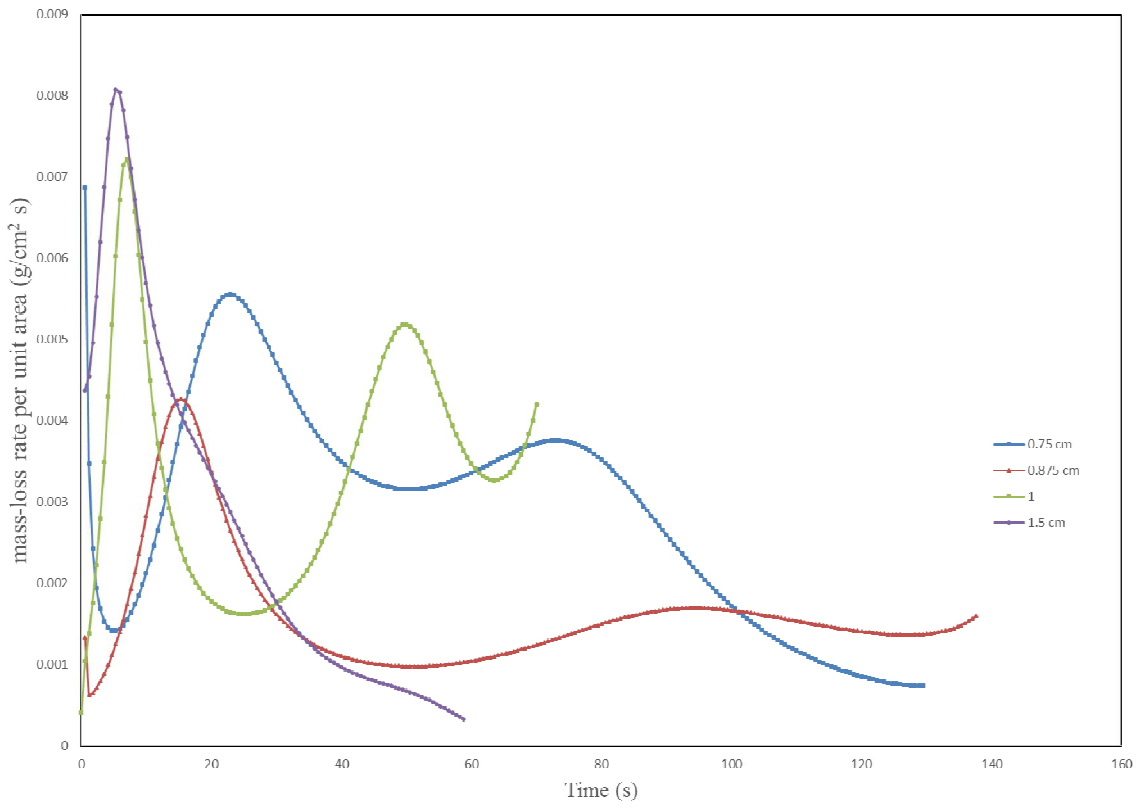


Figure A-3: Mass-loss rate per unit area

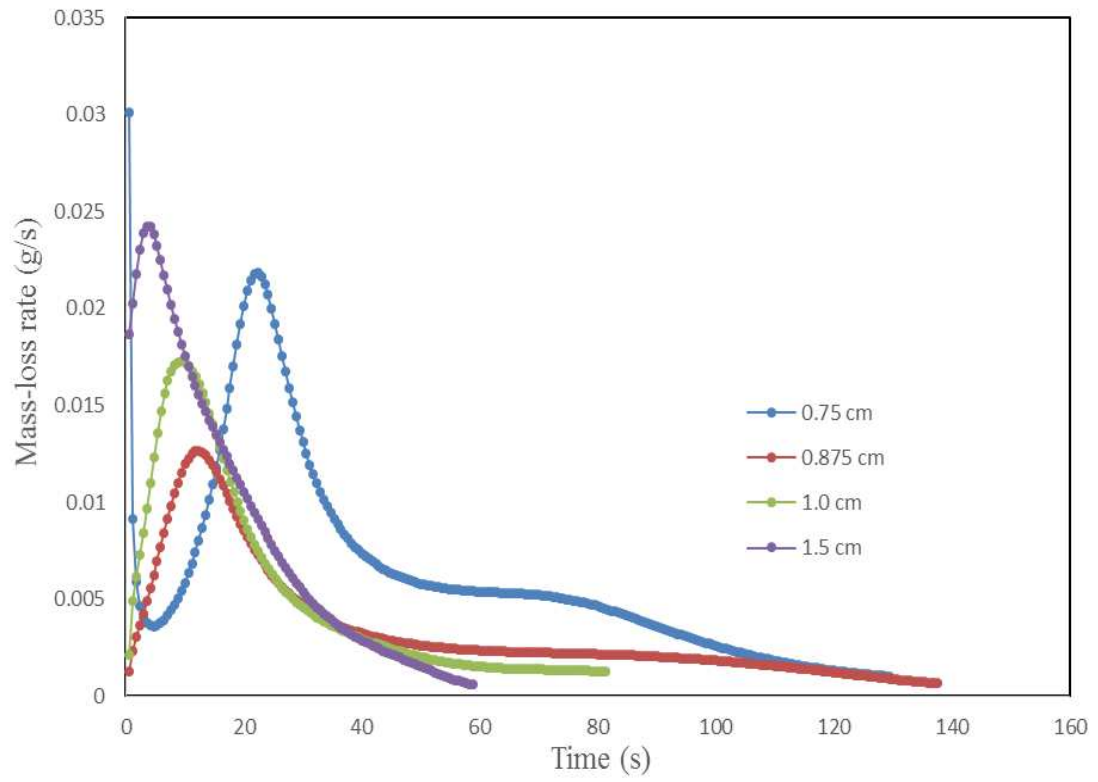


Figure A-4: Mass-loss rate per number of matchsticks ignited

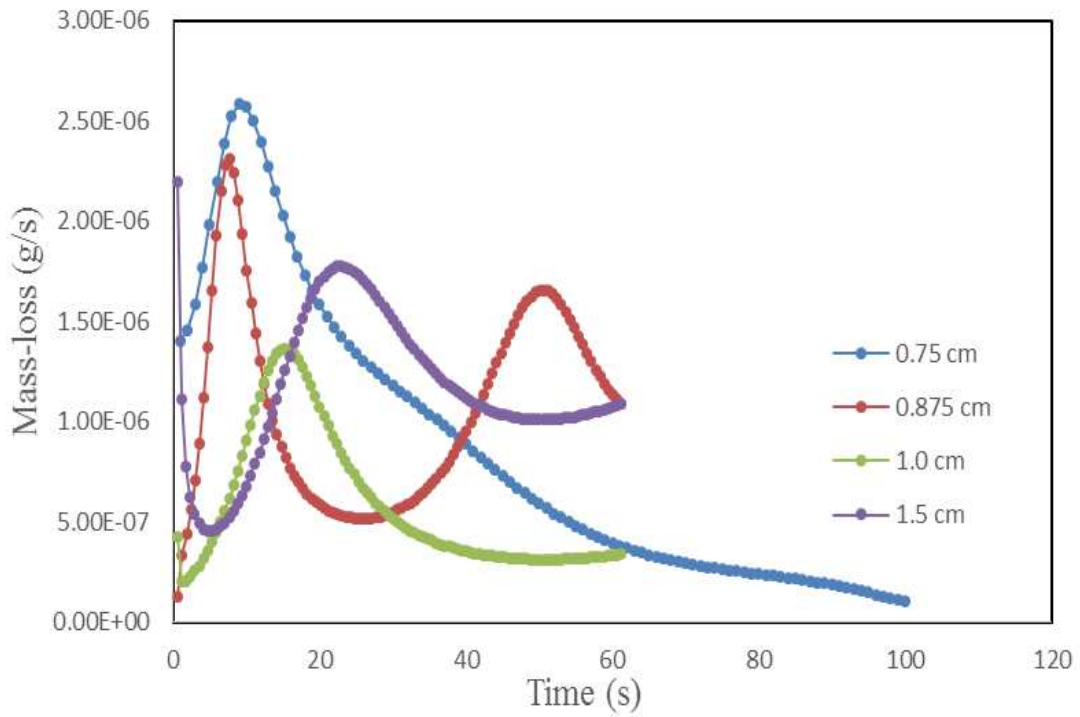


Figure A-5: Mass-loss rate per total number

## References

- [1] Emmons, H. W. (1980/81). The Growth of Fire Science. *Fire Safety Journal*, 95-106.
- [2] Gollner, M., Yanxuan, X., & Minkyu Lee, L. (2012). Burning Behavior of Vertical Matchstick. *Combustion Science and Technology*, 184: 585-607.
- [3] *Evaluation of Fire Models for Nuclear Power Plant Applications: Cable Tray Fires: International Panel Report*. Division of Risk Analysis and Applications, Office of Nuclear Regulatory Research, US Nuclear Regulatory Commission, 2002
- [4] Pryor, A. J. (1977). *The Browns Ferry Nuclear Plant Fire* . Boston: SFPE.
- [5] Finney, M. A., Jack D.Cohen, Sara S. McAllister, & W., M. (2013). On the need for a theory of wildland fire spread. *International Journal of Wildland Fire*, 22,25-36.
- [6] Comfort, K. H. (2014). *Dynamic decision processes in complex, high-risk operations: The*. Pittsburgh.
- [7] Quintiere, J. G. (2006). *Fundamentals of fire phenomena*. England: John Wiley.
- [8] Turns, S. R. (1996). *An introduction to combustion*. New York: McGraw-hill.
- [9] Jing Li, S. I. (2014). Measurement of kinetics and thermodynamics of the thermal degradation for charring polymers. *Polymer Degradation and Stability*, Volume 106, Pages 2-15.
- [10] Janssens, R. E. (2005). *Polymer Flammability* . Springfield: National Technical Information .
- [11] Drysdale, D. (2011). *An introduction to fire dynamics*. John Wiley & Sons
- [12] Ragland, K. W., Aerts, D. J, & Baker. , A. (1991). Properties of wood for combustion analysis. *Bioresource technology*, 161-168.

- [13] Serup, H., Falster, H., & Gamborg., C. (1999). *Wood for energy production. Technology-environment-economy*. Videncenter for Halm-og Flisfyring.
- [14] Annamalala, K., & Sibulkin, M. (1979). Flame Spread Over Combustible Surfaces for Laminar Flow Systems Part I: Excess Fuel and Heat Flux. *Combustion Science and Technology*, Volume 19, Issue 5-6.
- [15] Williams, F. A. (1977). Mechanisms of fire spread. *Symposium (International) on Combustion* , Vol. 16. No. 1.
- [16] Pagni, P. J., & Thomas, G. P. (1977). Flame spread through porous fuels. *Symposium (International) on Combustion*, 1099–1107.
- [17] Finney, M. A., Jack D. Cohen, Grenfelland, I. C., & Kara M, Y. (2010). An examination of fire spread thresholds in discontinuous. *International Journal of Wildland Fire* 2, 19,163-170.
- [18] Kashiwagi, T. (1975). A study of flame spread over a porous material under external radiation fluxes. *Symposium (International) on Combustion.* , Vol. 15. No. 1.
- [19] Zhao, Z., Daniel, G., & Gonller, M. (2013). Flame Spread through Arrays of Wooden Dowels.
- [20] Vogel, M., & Williams, F. (1970). Flame propagation along matchstick arrays. *Combustion Science and Technology*, 1(6), 429–436.
- [21] Weber, R. O. (1990). A model for fire propagation in arrays. *Mathematical and Computer Modelling*, 13.12: 95-102.
- [22] Fons, W. L. (1950). Heating and Ignition of Small Wood Cylinders. *Industrial and Engineering Chemistry*, Vol.42, No.10 2130-2133.
- [23] Emmons, H., & Shen, T. (1971). Fire spread in paper arrays. *Proc. Combust. Inst.*, 13(1), 917–926.
- [24] Prah, J., & Tien, J. (1973). Preliminary investigations of forced convection on flame. *Combustion Science and Technology*, 7(6), 271–282.

- [25] Hwang, C., & Xie, Y. (1984). Flame propagation along matchstick arrays on inclined base board. *Combustion Science and Technology*, 42(1), 1–12.
- [26] Emori, R. I. (1988). Simplified scale modeling of turbulent flame spread with implication to wildland fires. *Fire Safety and Science*, 2,263–273.
- [27] Weise, D., & Biging, G. (1994). Effects of wind velocity and slope on fire behavior. *Proceedings of the 4th international symposium on fire safety science*, 1041.
- [28] Hunter, L. (1979). Models of horizontal electric cables and cable trays exposed to a fire plume. *Combustion and Flame*, 32, 311-322.
- [29] Fernandez-Pellp, A,C, & Alvares, N. (2000). Fire initiation and spread in overloaded communication system cable trays. *Experimental Thermal and Fluid Science*, 21(1-3),51-57.
- [30] Fernandez-Pello, A., & Hirano. (1983). Controlling mechanisms of flame spread. *Combustion Science and Technology*, 32(1),1-31.
- [31] Marstrs.G.F. (1972). Arrays of heated horizontal cylinders in natural convection. *International Journal of Heat and Mass Transfer*, Volume 15, Pages 921-933.
- [32] Lee, C. (1978). Burning rate of fuel cylinders. *Combustion and Flame*, 32,271-276.